T H E U N I V E R S I T Y O F A L B E R T A

RELEASE FORM

NAME OF AUTHOR	Maxwell Larry Dupilka
TITLE OF THESIS	Natural Dipoles as a Source of Mountain-Associated-Infrasonic-Waves
DEGREE FOR WHICH THESIS WAS PRESENTED	Master of Science
YEAR THIS DEGREE GRANTED	1980

THE UNIVERSITY OF ALBERTA

NATURAL DIPOLES AS A SOURCE OF MOUNTAIN-ASSOCIATED-INFRASONIC-WAVES

by

(C) MAXWELL LARRY DUPILKA

A THESIS

SUBMITTED TO THE FACULTY OF GRADUATE STUDIES AND RESEARCH

IN PARTIAL FULFILMENT OF THE REQUIREMENTS FOR THE DEGREE

OF MASTER OF SCIENCE

IN

METEOROLOGY

DEPARTMENT OF GEOGRAPHY

EDMONTON, ALBERTA

FALL, 1980

THE UNIVERSITY OF ALBERTA

FACULTY OF GRADUATE STUDIES AND RESEARCH

The undersigned certify that they have read, and recommend to the Faculty of Graduate Studies and Research, for acceptance, a thesis entitled "Natural Dipoles as a Source of Mountain-Associated-Infrasonic-Waves" submitted by Maxwell Larry Dupilka in partial fulfilment of the requirements for the degree of Master of Science in Meteorology.

ABSTRACT

Sound waves of an unknown origin have been observed to radiate from specific areas in the Rocky Mountains. This prompted early researchers to refer to them as Mountain-Associated-Waves or MAW. These waves travel at sub-sonic frequencies (oscillation periods 1.0 to 1000 seconds) and are detected through a network of receivers located thousands of kilometers apart. The MAW events were found to be associated with areas of maximum wind in the upper atmosphere. This suggests a production mechanism which may depend on the speed of the air flow past the mountains.

A simple dipole model has been used to investigate the generation of MAW. Based on the theory of airflow around cylinders, but modified by incorporating laboratory results, the model has been extended to serve on a synoptic scale. In this "natural" dipole model the cylinder has been replaced by the massif of a mountain.

The observed MAW events were found to have preferred azimuthal ranges at a given receiving station. This may be due in part to the "steering" influence of the atmosphere upon sound wave propagation.

When the predicted events were compared to observations, it was found that the observed events were too small in number to warrant any definite conclusions. However, the natural dipole appears to be a possible explanation in over 50 percent of the cases studied.

ACKNOWLEDGEMENTS

I wish to express my sincere thanks to my departmental supervisor, Dr. E.R. Reinelt for having suggested this study and for his instrumental advice in preparing this thesis.

I would also like to thank Dr. K.D. Hage and Dr. A.N. Kamal who, along with Dr. Reinelt, served on my examining committee.

This thesis is based on original work begun by Professor L.B. Craine of Washington State University, Pullman, Washington along with Professor J.E. Thomas at the University of Idaho, Moscow, Idaho.

Special thanks is extended to Dawn Byrne for her expert typing skills.

This thesis was completed in part, while on educational leave from the Canadian Atmospheric Environment Service.

TABLE OF CONTENTS

LIST OF TABLES

LIST OF FIGURES

LIST OF SYMBOLS

SYMBOL		FIRST USED ON PAGE
B	barometric pressure	26
c	phase velocity	8
c_g	group velocity	25
c_h	horizontal trace velocity	25
c_s	signal velocity	25
c_p, c_v	specific heat of air at constant pressure and volume respectively	24
d	diameter of cylinder, diameter of mountain peak	9
f	frequency, Coriolis parameter	9
$f(R)$	a function of the Reynolds number	13
g	acceleration due to gravity	49
h	horizontal spacing of vortices	10
H	horizontal distance between contours on a constant pressure surface	49
i_j	angle of incidence	29
I	intensity	13
l	length of cylinder	13
r	distance from the source to the receiver	13
r_j	angle of refraction	29
Re	Reynolds number	9
R_m	specific gas constant for air	24
S	Strouhal number	9
T	temperature	24
U	wind speed	13
y	effective height of a mountain peak	51

SYMBOL		FIRST USED ON PAGE
Z	height above the Earth's surface	49
α_i	angle between arrival azimuths	49
β	angle of incidence	25
γ	lapse rate	29
θ	angle between the wind vector and the radius vector to the receiver	13
θ'	$90^{\circ} - \theta$	13
λ	wave length of vortices	10
μ	dynamic viscosity of air	9
ν	kinematic viscosity of air	9
ρ	density of air	9
τ	oscillation period	26
ϕ	latitude	49
ω	angular frequency	25
Ω	angular velocity of the Earth	49

CHAPTER 1

INTRODUCTION

1.1 Purpose of Study

The low-frequency band of of the acoustical spectrum below 15 Hz is generally referred to as the infrasonic region. There are a number of atmospheric wave structures travelling at acoustic velocities in the 10 to 100 second period range. Infrasound in this region has been indentified as coming from man-made sources such as nuclear explosions (Donn and Ewing, 1962) and sonic booms (Goerke, 1971). Various natural sources of infrasound include exploding meteors (Pekeris, 1948), volcanic explosions (Goerke, et al, 1965), earthquakes (Cook and Young, 1962), certain auroral events (Campbell and Young, 1963; Maeda and Young, 1966), and severe storms (Bowman and Bedard, 1972).

In addition to these infrasonic emissions, naturally occurring infrasound of unknown origin is frequently detected. Work by Greene and Howard (1975) indicates that these signals occur mainly in winter in the Northern Hemisphere. Location of a source requires triangulation from two or more observatories. The azimuth range for each station receiving these unknown signals shows some predominant bands. There is a clear tendency for the source locations to lie in rugged mountainous areas. This prompted early investigators to refer to these signals as "Mountain-Associated Waves" (MAW).

Fig. 1.1 shows the observed distribution of azimuth angles at Edson, Alberta. The predominant signal occurs along azimuths between 280° and 320°, suggesting the Rocky Mountains for possible source locations.

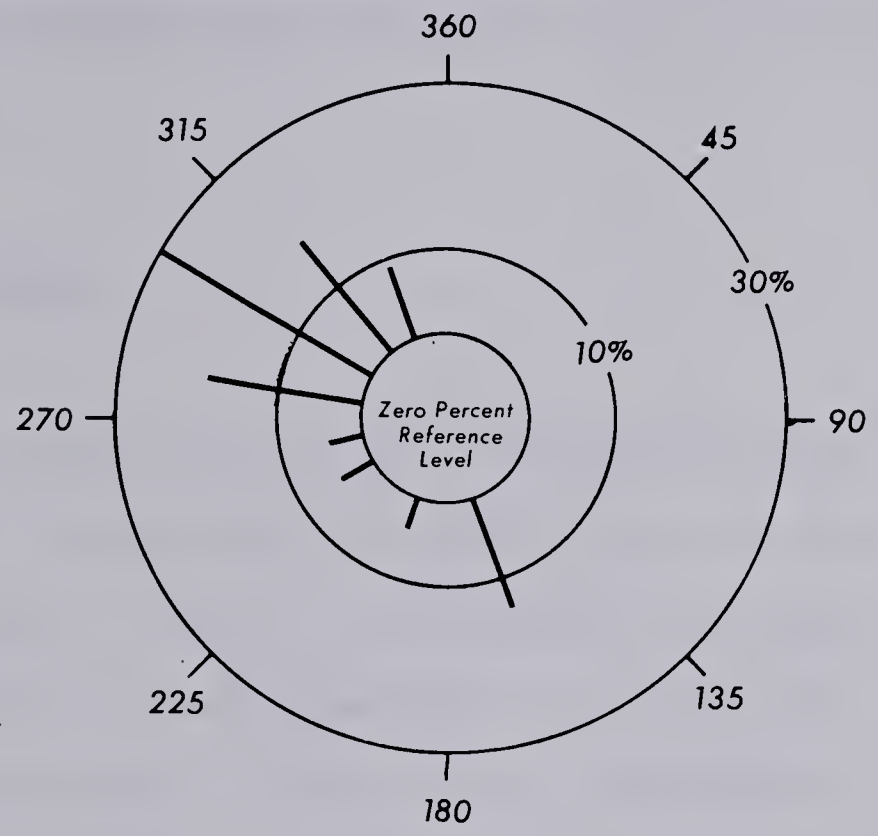

Fig. 1.1 Directions from which Infrasonic Waves are received at Edson, Alberta

The length of time during which MAW signals are continuously received (often called an "event") at a station varies from hours to days. Variations in signal characteristics during an event indicate that atmospheric parameters change over the course of observation, the nature of the source changes, or that two or more sources may be contributing to the signal.

Craine, Thomas (1970A, 1970B, 1971), and co-workers at Washington State University and the University of Idaho have for several years investigated natural aerodynamic sound as a likely source of Mountain-Associated Waves. Larsen (1971) has also suggested the interaction of winds with mountainous regions to be a possible source mechanism.

1.2 Proposed Theory

This thesis will attempt to show that natural aerodynamic sound of dipole origin is a likely source for many of the observed MAW events. A model for the production of sound at infrasonic frequencies in the atmosphere will be constructed. Propagation effects will be discussed to point out the difficulties involved in determining the origin of a sound ray emitted by a source of uncertain location.

The characteristics (ie. azimuth of arrival and intensity) of the sound received at an observatory on a given day are predicted. A triangulation region is constructed based on the model and then compared to actual observations for the same time period. Conclusions are then drawn according to the correlation between predicted and actual measurements.

CHAPTER II

AERODYNAMIC SOUND

2.1 Theory of Sound Production

Following the outline of acoustical theory and nomenclature given by Bates and Stevens (1966) and Kimpo (1973) there are three fundamental ways in which kinetic energy may be converted into infrasonic wave motion, namely through the action, respectively, of monopole, dipole and quadrupole oscillators.

2.1.1 Monopole

A monopole, sometimes called also a simple source, is produced by forcing the mass in a fixed region of space to fluctuate. One could picture a pulsating sphere which causes density fluctuations in the surrounding fluid, as shown schematically in Fig. 2.1a. The density fluctuations then propagate radially outward in the form of sound waves, producing a spherically symmetrical intensity field. Since the inward and outward fluctuations involve the same mass flux, there is no net momentum change.

2.1.2 Dipole

Forcing the momentum in a fixed region of space to fluctuate or, equivalently, forcing the rates of mass flux across fixed surfaces to vary constitutes a dipole (See Fig. 2.1b). Fluctuation of momentum corresponds to a fluctuation of force causing a density variation in the surrounding fluid which propagates away from the dipole in the

form of a sound wave. Physically, a dipole may be thought of as two monopoles, joined by a fixed axis, pulsating 180 degrees out of phase. The intensity of the sound field produced by a dipole is a maximum along the axis, decreasing to zero perpendicular to the axis (Fig. 2.1b).

2.1.3 Quadrupole

An acoustic quadrupole is equivalent to two dipoles acting together. The two dipoles can be thought of as two forces a small distance apart which cause a fluctuating shear stress within a fluid. The intensity field produced by a quadrupole (see Fig. 2.1c) has maxima along lines x and y, and minima along lines xx and yy.

The monopole, dipole and quadrupole form a monotonic sequence of decreasing efficiency in the sense that:

(a) a dipole is a less efficient means of energy conversion than a monopole, and a quadrupole is less efficient than a dipole.

(b) the differences in decreasing efficiency become more pronounced as the frequency of oscillation decreases.

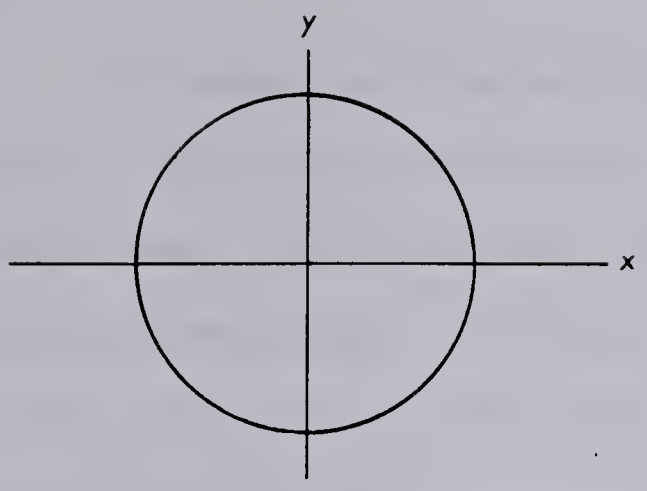

Fig. 2.1a

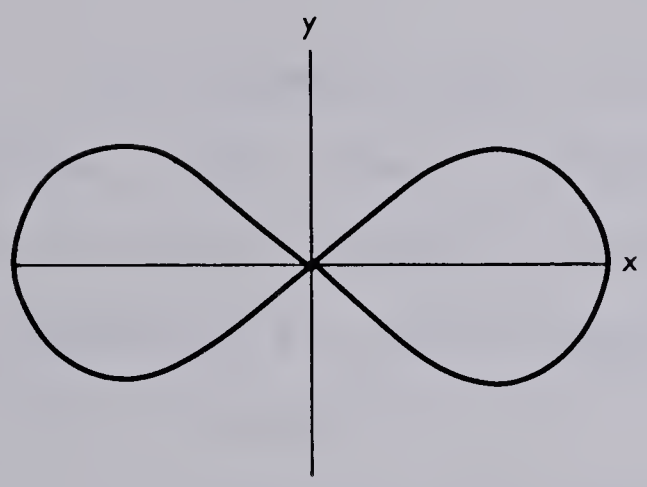

Fig. 2.1b

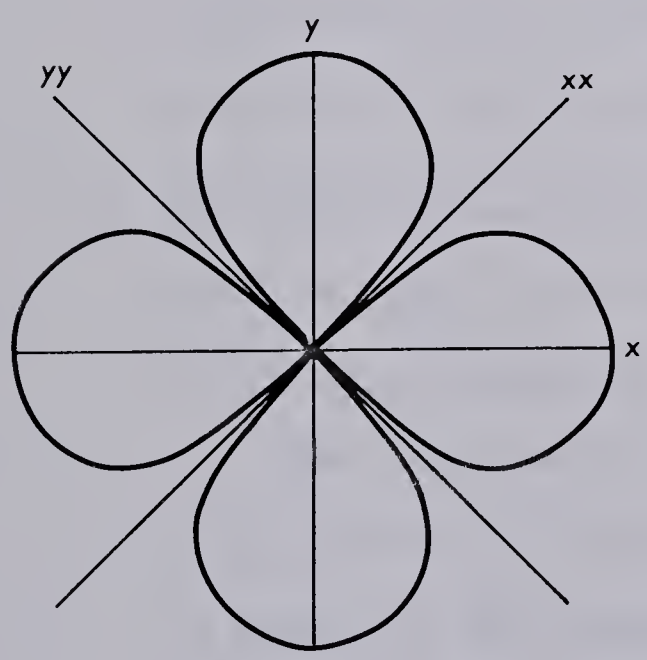

Fig. 2.1c

Fig. 2.1 Intensity field of sound produced by a) monopole, b) dipole, and c) quadrupole.

2.2 Aerodynamic Sound Production

2.2.1 Sound Field Characteristics

The production of sound in a free fluid, ie. a fluid not constrained by, nor containing within it, any solid boundaries, will be considered next. Sound produced in the absence of any solid boundaries is called aerodynamic sound. The first theory which concerned itself with the intensity of sound produced by a fluctuating fluid flow was developed by Lighthill (1951).

The stresses produced in the fluid give rise to a quadrupole type radiation field. Although Lighthill's theory assumes that there are no solid boundaries present, he pointed out that they might well play an important role in sound production, and could make their presence felt in two ways:

1) Sound generated by quadrupoles will be reflected and diffracted by solid boundaries.

2) The quadrupoles will be no longer distributed over the whole of space, but only throughout the region external to the solid boundaries.

   There may also be a resultant distribution of dipoles at the solid-fluid interface. (Dipoles are likely since, in acoustics, they correspond to externally-applied fluctuating forces, and such forces are present between the fluid and solid boundary).

Curle (1955) extended Lighthill's theory by examining the influence of solid boundaries upon the production of aerodynamic sound. He showed that the sound field may be regarded as being derived from two distinct origins:

1) the quadrupole field which represents the fluctuating applied stresses within the fluid;
2) the dipole field, which represents the fluctuating force with which the solid boundaries act on the fluid.

The relative magnitude of dipole and quadrupole radiation intensities is given as:

$$\frac{I_Q}{I_D} \alpha \left(\frac{U}{c}\right)^2 \quad \text{x function of the Reynolds number} \qquad (2.1)$$

Thus for a sufficiently small Mach number (U/c), the contribution to the sound field from the dipoles should be greater than from the quadrupoles. The exact value of Mach number for this to occur depends upon the nature of the function of the Reynolds number, which in turn is determined by the characteristics of the flow.

2.2.2 Flow of Air Past a Cylinder

A stationary cylinder embedded in an air stream, with its axis perpendicular to the flow may be expected to cause quadrupole and dipole acoustical fields to be set up. Before examining the characteristics of the sound field produced in such a manner, it is useful to review the concept of the Reynolds number.

The nature of a flow, ie. whether it is laminar or turbulent, and its position on a scale indicating the relative importance of laminar to turbulent tendencies is indicated by the Reynolds number, a non-dimensional quantity defined as:

$$Re = \frac{\text{inertial forces}}{\text{viscous forces}} = \frac{Ud\rho}{\mu} \qquad (2.2)$$

Defining the kinematic viscosity by $\nu = \frac{\mu}{\rho}$, the Reynolds number may be written as:

$$Re = \frac{Ud}{\nu} \qquad (2.3)$$

2.2.2.1 Kármán vortices and Strouhal Number

The first extensive experiments on the flow of air past a stationary circular cylinder were done by Strouhal (1878). He found that sound of an essentially pure tonal character is radiated for Reynolds numbers in the range of 50 to 3×10^4. Such sounds are usually referred to as "Aeolian tones", and are familiar as the "humming" of telephone or power lines in high winds. Strouhal found that the frequency of the note was predicted by:

$$f = 0.185 \frac{U}{d} \qquad (2.4)$$

It is now customary to express the frequency in terms of the non-dimensional Strouhal number, S, such that:

$$S = \frac{f\,d}{U} \qquad (2.5)$$

($S = 0.185$ in Strouhal's experiments)

Since Strouhal's early findings, there have been numerous experiments dealing with flow past cylinders in an attempt to explain the production of aeolian tones. A significant advancement occurred when Von Kármán (1911) developed his now-famous theory of the "vortex street". The basic vortex theorem states that the fluid flow across a cylinder will result in the formation of two unsymmetrical rows of vortices with alternating arrangement (Fig. 2.2).

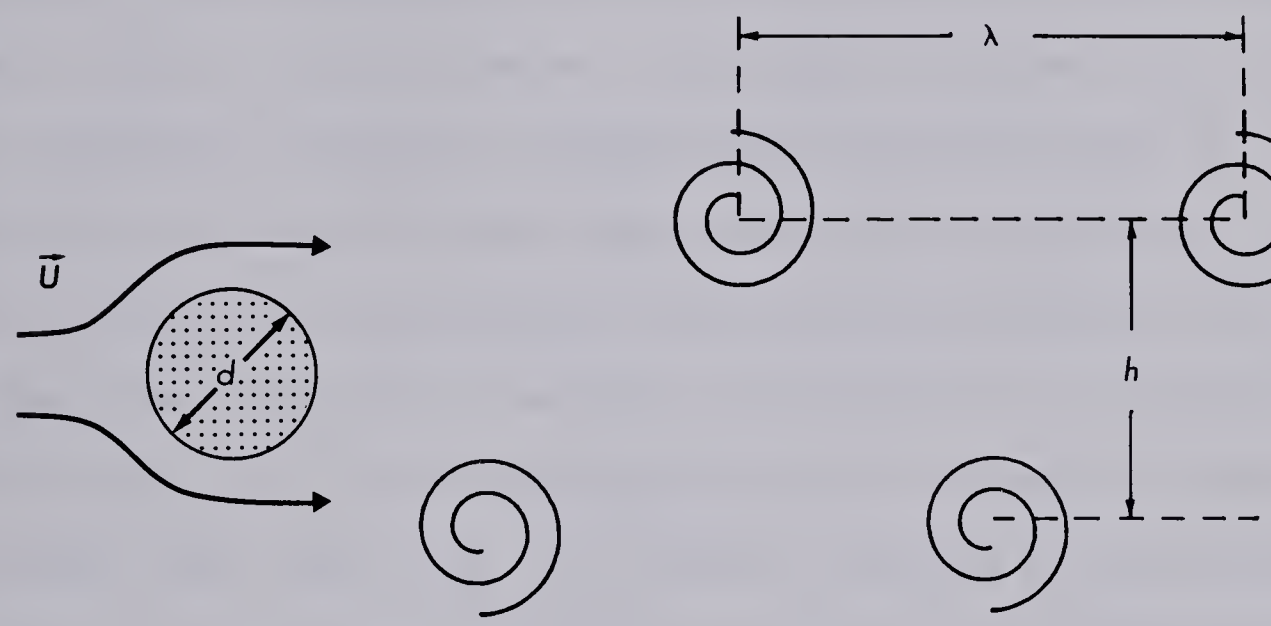

Fig. 2.2 Production of Kármán vortices in the wake of a cylinder

According to this theory, an arrangement of two rows of vortices is unstable unless they are positioned in accordance with the spacing ratio given by:

$$\frac{h}{\lambda} = 0.28 \qquad (2.6)$$

This phenomenon of vortex shedding is responsible for the production of aeolian tones; the frequency of the tone emitted is equal to the rate at which the vortices are shed.

Since Von Kármán's original work, many theoretical and experimental investigations on the Kármán vortex street have been conducted (eg. Roshko, 1954a, 1954b and 1961, Gerrard, 1966). Although very little is understood about the principles involved in the actual vortex shedding at the cylinder, some interesting results have been obtained. For example, it was originally thought that organized vortex shedding occurs only over a rather limited range of Reynolds numbers($50 < Re < 10^5$). Laboratory results have shown, however, that it exists to Reynolds numbers of at least 10^7 (Roshko, 1961) and there appears to be no reason to believe that this is an upper limit. However, it is extremely difficult to produce higher Reynolds numbers in a laboratory, so results in this higher range remain unavailable. Another result has been the determination of the frequency with which the vortices are shed from the cylinder, and hence the frequency of the sound produced. As mentioned earlier, this frequency is usually expressed in terms of a Strouhal number (Eqn. 2.5). The Strouhal shedding frequency appears to be about 0.28 for circular cylinders at high Reynolds numbers (Roshko, 1961), decreasing to about 0.18 at low Reynolds numbers (Gerrard, 1955).

It should be noted that the frequency of the sound produced by the shedding of vortices is independent of temperature, density and composition of the fluid.

For circular cones the frequency is determined by the local diameter and there is a spanwise coupling of frequencies along the length of the cone (Gaster, 1969). Instead of observing a single

frequency, or pure tone, as in the case for cylinders, one could expect a broadening of the spectrum. This effect becomes increasingly important at lower frequencies.

2.2.2.2 Sound Field

Theory shows that the fluctuating forces of an air flow on a rigid body may be expected to possess an associated dipole radiation field (Lighthill, 1952). Experiments have confirmed this (Gerrard, 1955). The sound field produced by an air flow past a cylinder, perpendicular to the axis, is found to possess a dipole field (Fig. 2.3) of nearly pure tone character; the harmonics present are considerably less intense than the fundamental frequency (Etkin, 1957).

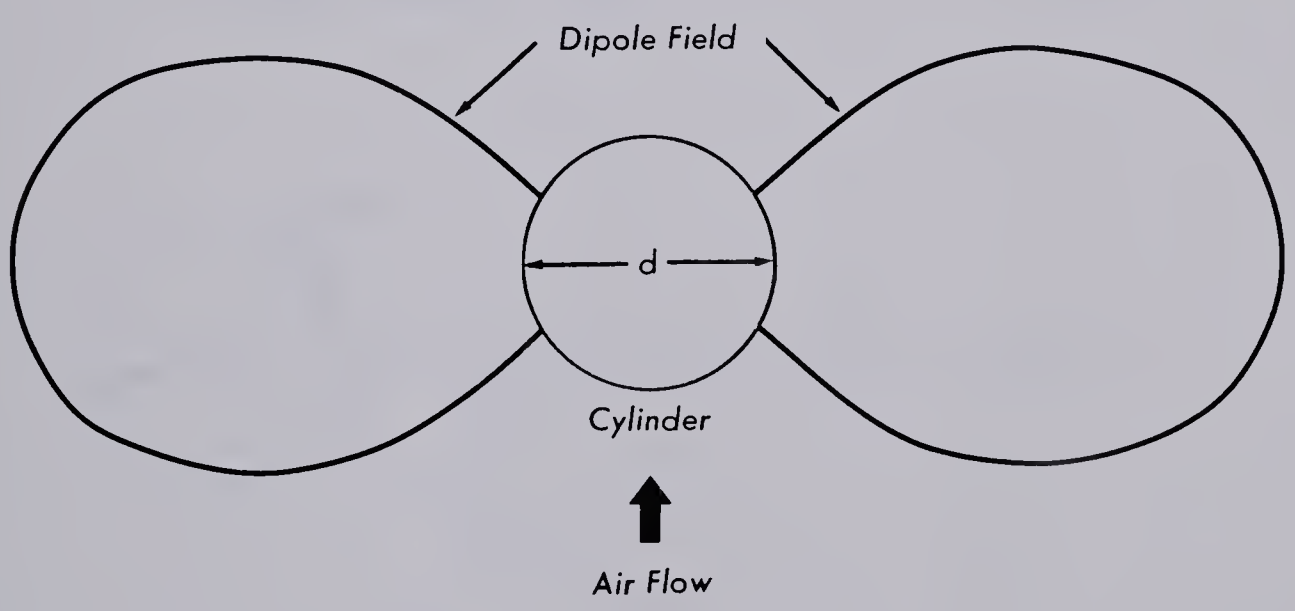

Fig. 2.3 Resulting dipole field formed by a cylinder embedded in a flow of air.

The sound generated is aerodynamic, ie. it is not produced by vibration of the cylinder itself. The sound spectrum has a strong peak at the fundamental frequency, a weak peak at double the fundamental

frequency and wide-band noise at higher frequencies. The wide-band noise appears to originate from quadrupole sources produced in the wake of the cylinder. The fundamental tone radiates most strongly in a direction perpendicular to the flow, while the weak harmonic radiates most strongly parallel to the flow. The sound produced shows no dependence upon the physical properties of the cylinder (eg. type of material, hollow vs. solid cylinder).

2.2.2.3 Intensity Field

Experiments suggest (Gerrard, 1955) that at large distances from the cylinder axis ($\frac{r}{l} > 1$) in an air flow of velocity U, relative to the cylinder, the intensity of the sound obeys the relation:

$$I = \frac{U^4 l^2 \rho}{c r^2} \cos^2 \theta' \quad f(R) \qquad (2.7)$$

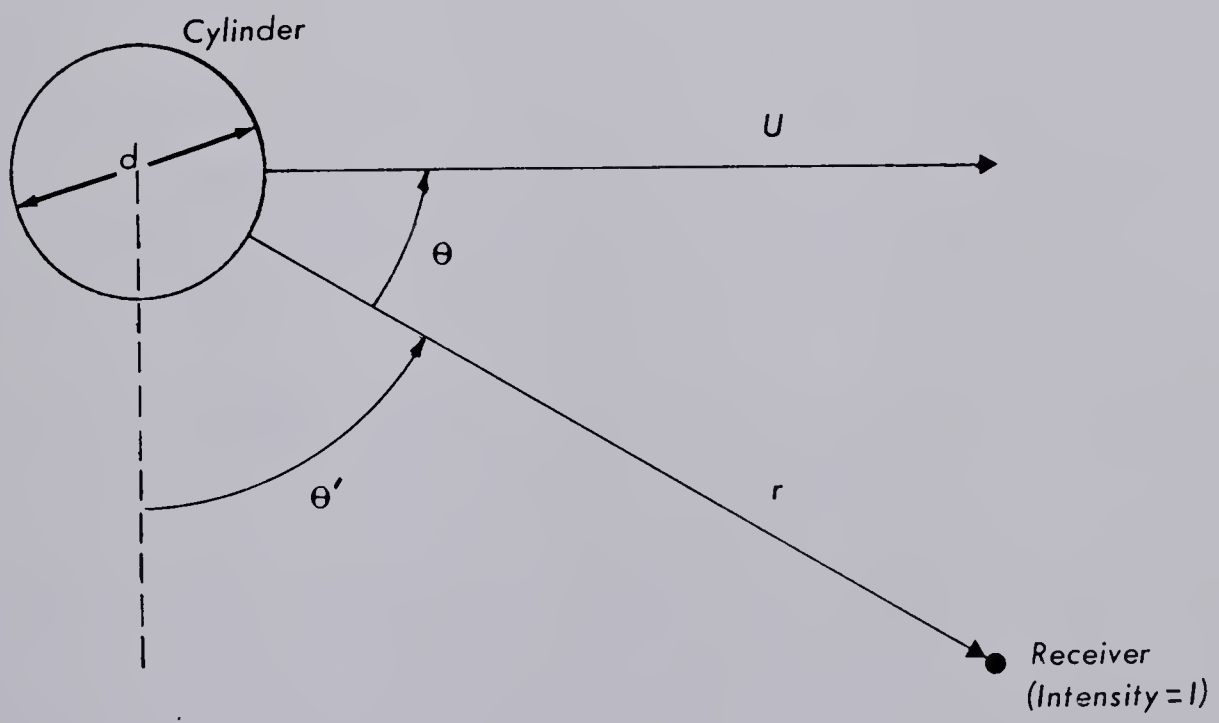

Fig. 2.4 Intensity at a distance r from the cylinder axis

The intensity is independent of the elastic properties of the cylinder (ie. cylinders of steel and brass, as well as hollow cylinders produced the same intensity for all other parameters remaining constant). Holle (1938) investigated the dependence of sound intensity upon the velocity for various values of cylinder diameter. He found no dependence on diameter except at high velocities ($U > 30$ m/sec).

CHAPTER III

PRODUCTION OF MOUNTAIN-ASSOCIATED WAVES

3.1 Natural Dipole Generators

The flow of air past a stationary cylinder may be intuitively extended, on a global scale, to the flow of air past a prominent mountain peak, with an accompanying conversion of kinetic to acoustic energy. A dipole radiation field will be produced in similar manner to that produced by a cylinder. The mountain-associated waves can now be thought of as a form of aeolian tones in the infrasonic frequency range.

Although there is little theoretical or experimental evidence to support this theory for the production of mountain-associated waves, some authors have suggested such a means of production, and the need for work in this area (Larson, 1971, Gossard and Hooke, 1975). The Von Kármán vortex street has been observed in the wake of mountain peaks with the aid of satellite photography (NASA, 1967).

A splendid example of the natural occurrence of vortex shedding on a synoptic scale, with Reynolds numbers far greater than can be achieved in a laboratory ($Re \sim 10^{10}$), is given by Teunissen (1977). By reconstructing the flow pattern, Teunissen obtains a Reynolds number of 5.2×10^9 and a Strouhal number of 0.15. The latter value agrees well with Strouhal numbers obtained in laboratory experiments. Recall

that Von Kármán concluded the vortex street would remain stable only if the ratio h/λ were equal to 0.28. Teunissen calculates a value of h/λ to be 0.3.

Photographs of vortex streets on a synoptic scale have become fairly familiar in recent years (eg. Bayliss, 1976). The importance for the existence of vortex streets on synoptic scales comes to the fore when one recalls that aeolian tones are produced by the breaking away of vortices. Just as acoustical aeolian tones are detected, for example, as the humming of power lines in the wind, infrasonic aeolian tones may exist as MAW.

Teunissen (1977) has calculated a vortex shedding frequency of 10^{-4}/sec for the flow of air past a mountain that is 1300 m high. Recalling the theory states that the sound frequency is equal to the vortex shedding frequency, this implies a sonic frequency of 10^{-4} Hz , certainly well into the infrasonic range.

If mountain-associated waves are actually produced by a natural dipole it would be a main source since, after a simple source, the dipole is the next most efficient method of converting kinetic energy to acoustical energy.

3.1.1 Dipole Model

This model deals with one type of natural dipole source in the atmosphere, the flow of air past a mountain peak. Two conditions are necessary: a mountain of large diameter projecting well above the

surrounding lesser peaks, and an appropriate flow of air. Rather than working with every mountain in a given region, only the most prominent peak is considered in the analysis.

There are ten mountain regions in the area under study (Fig. 3.2 and Table 3.1). The resolution possible from topographical maps enabled a boundary to be drawn for each of the regions. These source locations need only be checked for wind speed and direction to provide input for the dipole model.

3.1.1.1 Frequency of Mountain-Associated Waves

For atmospheric flow past a mountain the Reynolds number is typically around 10^9. For very high Reynolds numbers such as these, the corresponding Strouhal number appears to be about 0.27 (Roshko, 1961). A check can be made on the reasonability of the frequency prediction by using Strouhal's Law. The actual frequencies are known (.01 Hz<f<.1 Hz), S is known, U can be obtained from upper-air charts, d can be derived and then checked, using topographical maps, as being of reasonable value. For typical values of U and f, d has a value of about 500 meters; there is, therefore, no need to perform this check in each instance. (Note that d is now the diameter of a mountain peak).

3.1.1.2 Intensity of Mountain-Associated Waves

Equation 2.7 introduced in the previous chapter will be used to predict the intensity of the mountain-associated waves at a receiving station.

The function, f(R), has only been obtained for Reynolds numbers up to 10^4 (Gerrard, 1955). In this range it has the form:

$$f(R) = 3.6 \times 10^9 \, (Re)^3 \qquad (3.1)$$

Since there has been little experimental work done at higher Reynolds numbers, the above functional relation for f(R) will be extended and applied to atmospheric flows.

Substituting for Re $\left(= \frac{U\,d}{\nu}\right)$, equation 2.7 becomes:

$$I = (3.6 \times 10^9) \frac{d^3 U^7 y^2 \rho}{c \nu^3 r^2} \sin^2\theta \qquad (3.2)$$

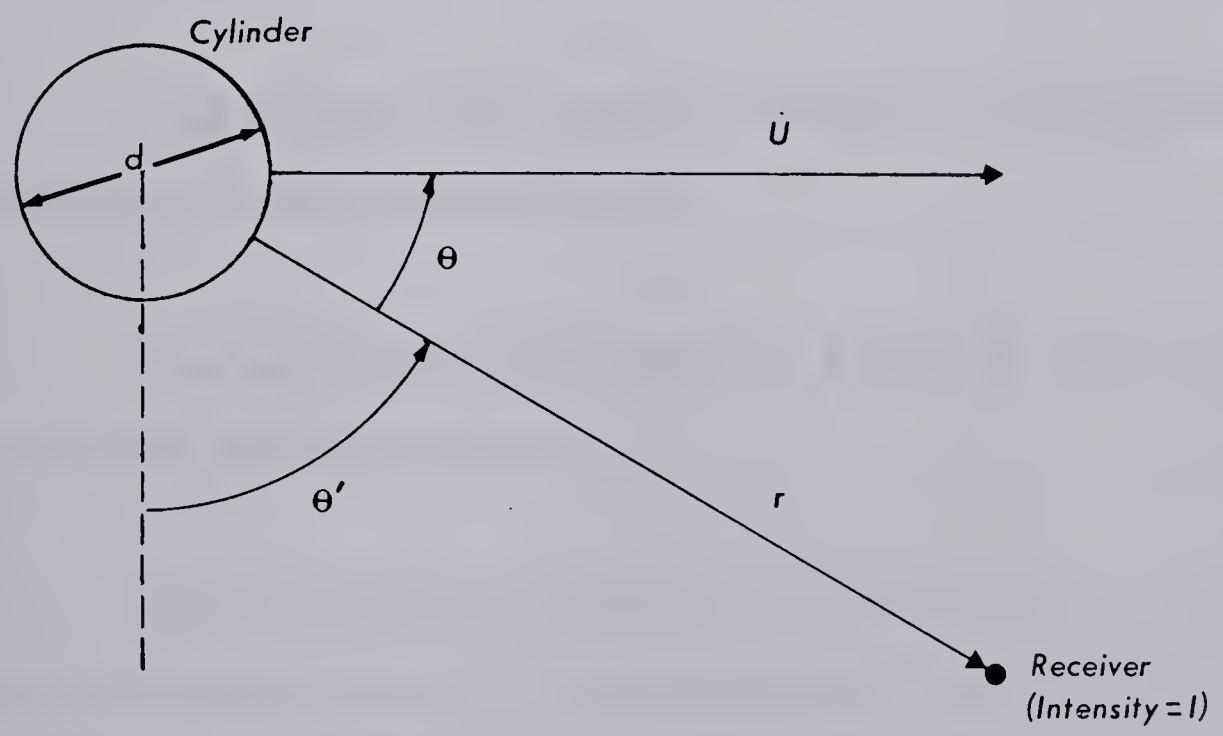

Fig. 3.1 Intensity at a distance r from a source of diameter d in a flow of velocity U

An explanation of the variables and the procedure for obtaining their values follows.

The peak diameter, d, can be obtained from Strouhal's law, or by use of a topographical map. A value of 500 m has been found to be a reasonable estimate for most mountain peaks.

The determination of the physically significant height of the peak, y, poses a problem; should y be measured from sea level, from the base of the mountain, or some other reference level. Since it is the interaction of an isolated peak with the wind that is important, the height, y, is taken as that portion of the peak which is above the average height of the surrounding terrain. A visual inspection of a topographical map shows the average height above sea level of the terrain to be about 2500 meters in Regions 1 to 9 and 3000 meters in Region 10. (Peak height, and height above sea level are given in Table 3.1).

The distance from source to receiver, r, is assumed to follow the great circle arc between the two.

The angle θ and wind speed U, as shown on Fig. 3.1, are obtained from upper-air charts.

The values of air density, ρ , sound velocity, c, and kinematic viscosity of air, ν , are calculated from meteorological observations (see Chapter VI).

The intensities at a receiving station from each of the sources can be ranked, and a dominant dipole generator picked out.

In summary, the dipole model predicts generation of infrasound whenever air flows past a mountain peak. The sound will be received at a station if the wind vector U and radius vector r (see Fig. 3.1) are not parallel, ie. $\theta \neq 0$ degrees. The sources will be ranked according to intensity.

TABLE 3.1

Prominent Mountains in Each of the Ten Regions

LOCATION	MOUNTAIN	HEIGHT ABOVE SEA LEVEL (m)	PEAK HEIGHT (m)	LAT. DEGREES NORTH	LONG. DEGREES WEST
1.	Mt. Robson	3954	1454	53	119
2.	Mt. Sylvia	2946	446	58	124
3.	Keele Peak	2972	472	63	131
4.	Mt. Isto	2761	261	69	144
5.	Mt. McKinley	6194	3694	63	151
6.	Mt. Logan	6050	3550	60	140
7.	Mt. Waddington	4042	1542	51	125
8.	Mt. Rainier	4392	1892	47	121
9.	Mt. Whitney	4418	1918	36	118
10.	Mt. Elbert	4399	1399	39	106

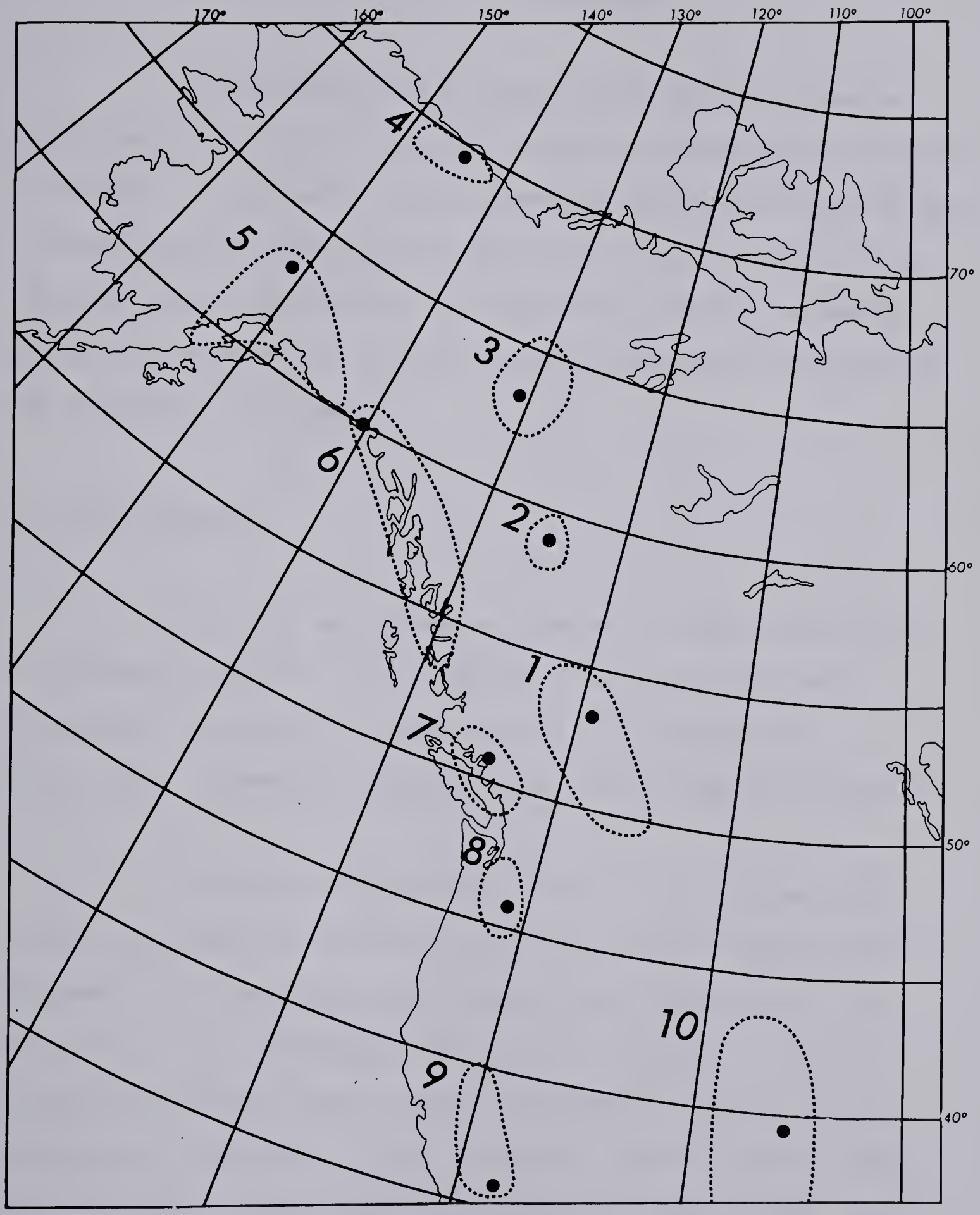

Fig. 3.2 Major mountain areas and highest peak in each area

CHAPTER IV

PROPAGATION OF SOUND IN THE ATMOSPHERE

The characteristics and state of the atmosphere have a significant effect on the infrasonic signal as it propagates from source to receiver. It may well be that propagation effects have more influence in determining the qualities of a signal at a receiving station than the variations at the sources. Although much is not yet understood concerning propagation of infrasound, some of the better-known effects are described in this chapter.

4.1 Sound Pressure

As a sound wave passes an observer it causes fluctuations in atmospheric pressure. For infrasound of natural origin these fluctuations are usually in the range of 0.1 to 100 dyne/cm^2 (Cook, 1969). Atmospheric pressure at sea level is about 10^6 dyne/cm^2.

Infrasound is detected by a series of microphones which convert the pressure fluctuations to variation of an electric current. The passage of a sound wave also produces small oscillations of the air particles and a subsequent variation in temperature. Hot-wire anemometers have been used to measure infrasound by means of these temperature fluctuations. Since microphones must be located out-of-doors, they also record variations not due to infrasonic waves. For example, turbulent eddies produce temperature and pressure variations.

Most infrasonic microphones are designed to respond to pressure rather than temperature variations, since this has been found to be the more reliable method.

4.2 Velocity of Infrasound

The speed of sound in air is:

$$c^2 = \frac{c_p}{c_v} R_m T \qquad (4.1)$$

Thus, the speed is proportional to the square root of the absolute temperature. (For air at a temperature of 20° C the speed of sound is about 344 m/sec.). This formula is applicable for all sound waves from the low infrasonic frequences (f = 0.001 Hz) to the high ultrasonic frequences (f > 20,000 Hz).

The literature on atmospheric sound usually distinguishes four different velocities and defines them as: (1) phase velocity; (2) group velocity; (3) signal velocity, and; (4) horizontal trace velocity.

The phase velocity, c, is the speed at which a surface of constant phase travels through a medium, ie. the atmospheric air. This velocity is a function of temperature. For horizontal propagation, where the temperature is relatively constant within a layer, the phase velocity is also nearly constant. For vertical propagation, where the variation of temperature is large, the phase velocity is a function of the temperature field.

The group velocity is defined as:

$$c_g = \frac{d\omega}{dk} \quad , \qquad (4.2)$$

where $\omega = 2\pi f$ is the angular frequency and $k = 2\pi/\lambda$ is the wave-number. It is the velocity at which the sound energy propagates through the medium.

The signal velocity is defined as:

$$c_s = \frac{D}{t} \quad , \qquad (4.3)$$

where D is the distance (from source to receiver) and t is the time of transit. In general, the phase, group and signal velocities are different and depend on the structure of the atmosphere.

The horizontal trace velocity, c_h , is the speed that is actually measured at an observing station, since infrasonic microphones are usually located on the Earth's surface and in the same horizontal plane. This velocity depends on the angle of incidence, β , of the sound ray such that $c_h = c \sin\beta$ (Fig. 4.1).

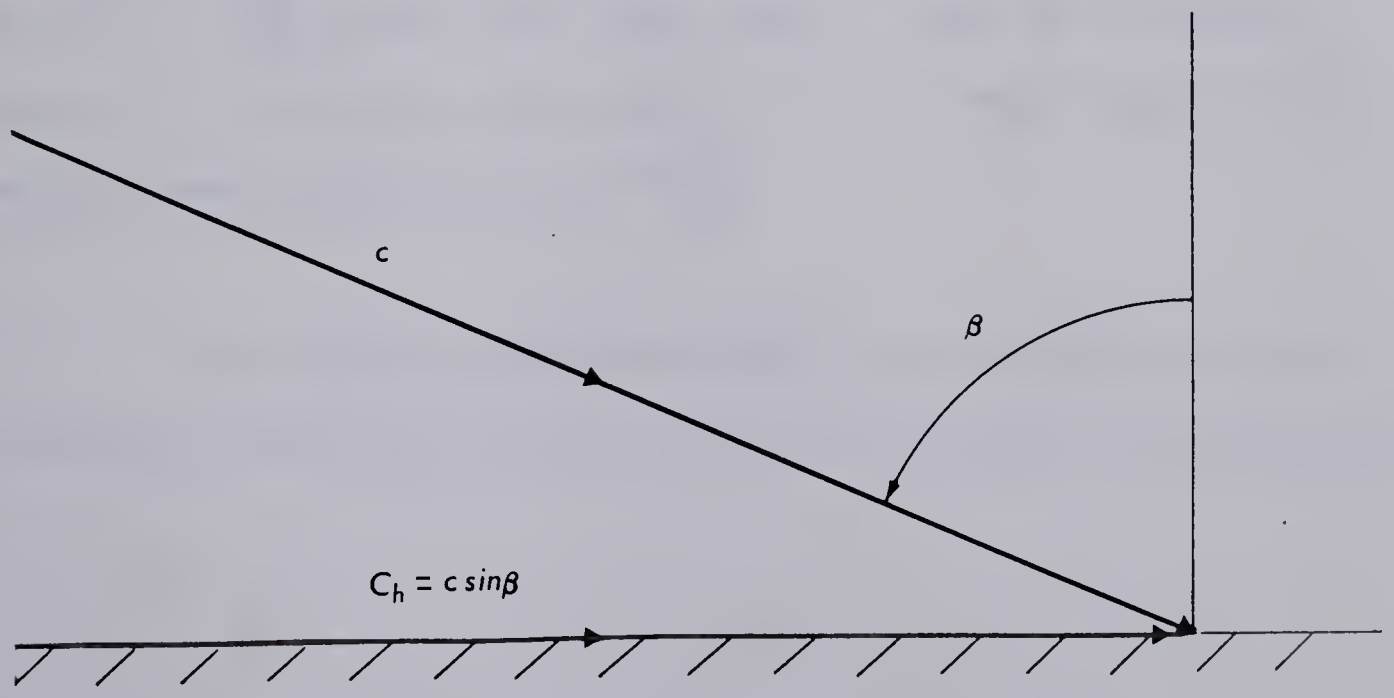

Fig. 4.1 For a plane wave of speed c, the horizontal trace velocity is c_h .

4.3 The Attenuation of Sound in the Atmosphere

There are four main factors in the atmosphere which contribute to the absorption of infrasound: viscosity, heat conduction, water vapor, and relaxation of thermal energy.

The attenuation of infrasound in the atmosphere due to viscosity and heat conduction is considerably less than for audible sounds because of the low frequency of oscillation. The absorption coefficient is about $1.6 \times 10^{-4} / \tau^2 B \frac{db}{km}$, where B is the barometric pressure in dyne/cm^2. For a plane wave in the lower atmosphere (ie. at altitudes below 90 km) at a period of $\tau = 10$ seconds, the absorption is less that $2 \times 10^{-9} \frac{db}{km}$ (Cook, 1962). Hence, the loss due to this effect is insignificant, even for propagation over distances of thousands of kilometers.

Below altitudes of 10 km the absorption due to water vapor may be expected to be significant. The exact variation of this absorption with atmospheric pressure is not accurately known for infrasonic frequencies. It is estimated to be as large as $5 \times 10^{-9} / \tau^2 \frac{db}{km}$ at sea level (Cook, 1962). Thus, for infrasonic levels at $\tau = 10$ seconds, the absorption due to water vapor is still insignificant, being only $5 \times 10^{-8} \frac{db}{km}$.

At very low frequencies there is an absorption due to relaxation of the thermal energy stored in vibrations of the diatomic

molecules in air. This is estimated to be about 10^{-6} $\frac{db}{km}$ for a wave of τ = 10 seconds, in the lower atmosphere (Cook, 1962). Again, this is a relatively small loss and of little importance in infrasonic transmission.

The absorption of infrasound in the atmosphere due to all four effects is thus small enough so that propagation can occur over large distances without any substantial loss in energy.

4.4 Temperature Effects

Since the refraction of sound waves in the presence of atmospheric temperature gradients is a well-known phenomenon, only a brief summary will be given here (See Fleagle and Businger, 1963).

The atmosphere may be imagined to be composed of a large number of quasi-horizontal layers, each differing in temperature from adjacent layers. Sound waves experience refraction at the boundaries between layers (Fig. 4.2).

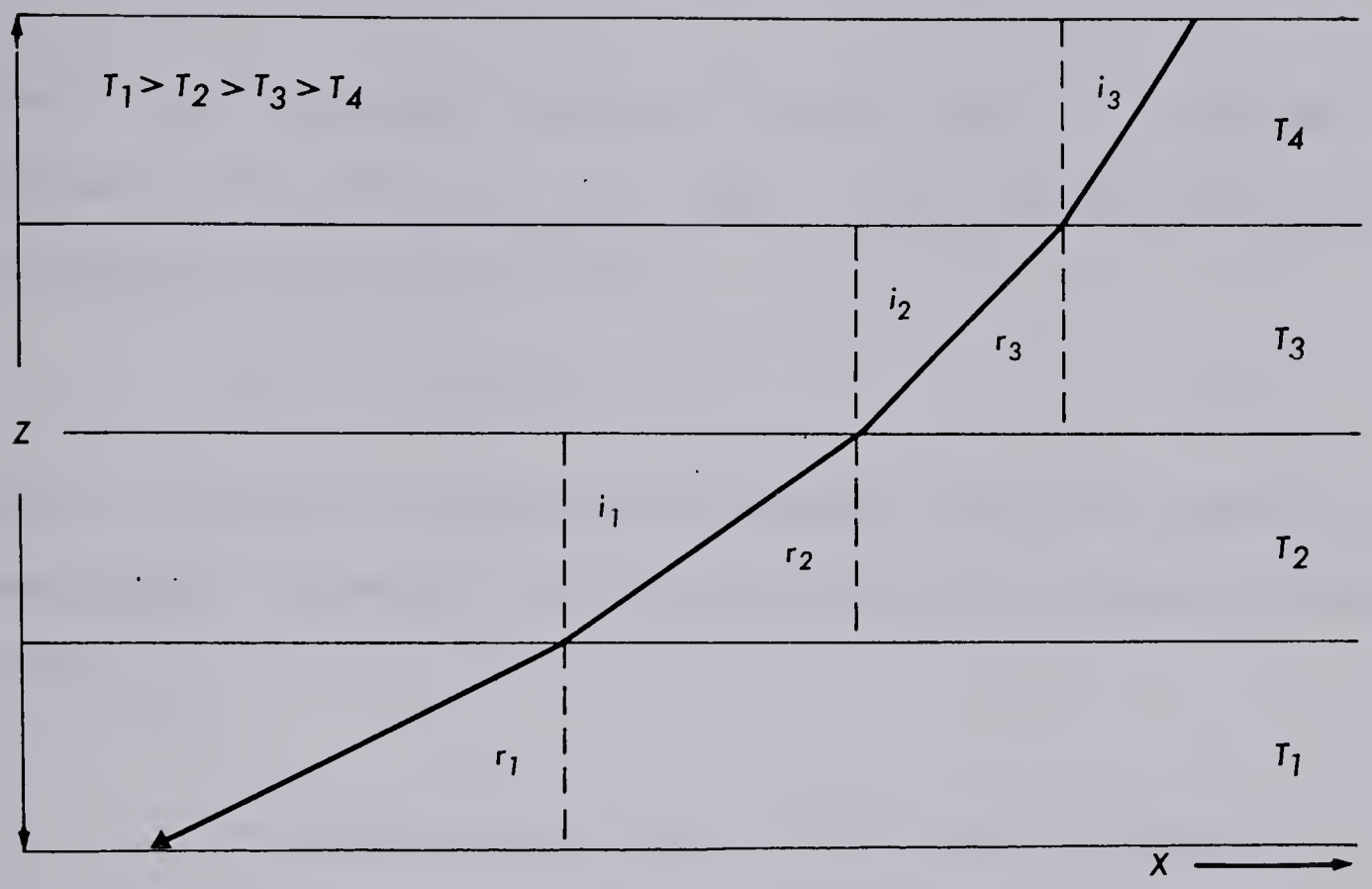

Fig. 4.2 Refraction of a sound ray due to vertical atmospheric temperature gradient.

Snell's law applies at each interface, such that:

$$\frac{\sin i_1}{c_1} = \frac{\sin r_1}{c_2} = \frac{\sin i_2}{c_2} \text{ , etc.} \qquad (4.4)$$

where c_n is the phase velocity of sound in layer n. Using the expression for velocity of sound (Eqn. 4.1) and assuming that $\frac{c_p}{c_v} R_m$ is constant along the ray gives:

$$\sin i = \text{constant} \times \sqrt{T} \qquad (4.5)$$

Hence, a decrease of temperature with height causes the sound ray to bend upward. Conversely, an inversion would cause a downward bending of the ray.

To evaluate the constant, T and i must be known at some point along the ray. For a ray which becomes horizontal at some point ($i = 90^{\circ}$) it is seen that:

$$\frac{\sin i}{\sqrt{T}} = \frac{1}{\sqrt{T'}} \text{ , or } \tan i = \sqrt{\frac{T}{T'-T}} \qquad (4.6)$$

where T' is the temperature at the point where the ray is horizontal. If the temperature is assumed to be a linear function of height such that $T = T' - \gamma z$, where T represents the absolute temperature at any reference height and γ is the lapse rate, then, with tan i replaced by dx / dz :

$$dx = \sqrt{\frac{T}{\gamma z}}\, dz \qquad (4.7)$$

This equation may be integrated numerically to calculate the path of a ray. It has been used in the original detection of the stratospheric temperature inversion.

About the time of World War I it became apparent that the sound of gunfire could be heard within a radius of about 100 km from the source and often beyond 200 km, but not at distances between 100 and 200 km. As shown in Fig. 4.3, within the central circle the wave was audible, but at greater radii upward refraction made the wave inaudible. However, at still greater radii beyond the zone of silence waves were refracted downward to ground level by a warm layer of air in the high atmosphere. It is now recognized that the temperature at 50 km above the surface in mid-latitudes may be on occasion as high as 325^{o} K (52^{o} C).

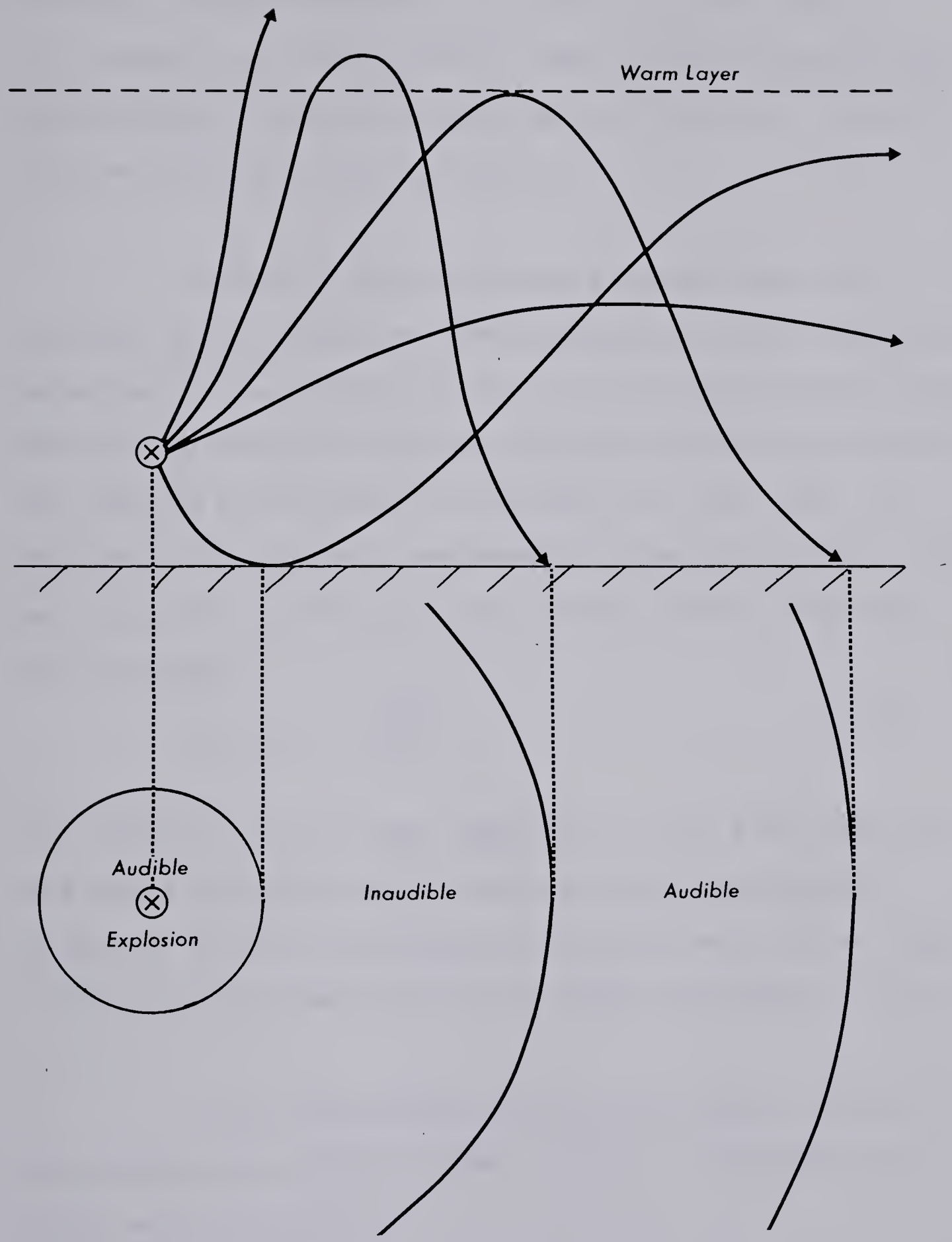

Fig. 4.3 (a) Propagation of sound from an explosion

(b) Audible and Inaudible zones

From the previous discussion it is clear that the infrasonic signals received at a station may not have travelled in a straight line from the source. Indeed, while one station may receive signals from a given source, another station at a somewhat different location may not receive them.

Infrasonic waves produced by a natural dipole are refracted away from the earth under conditions of normal atmospheric lapse rate. For any lapse rate there is a critical ray which strikes the earth horizontally; beyond this distance the only sound reaching the ground is due to scattering and usually very weak (Fig. 4.4). Equation 4.7 may be used to determine the maximum range of the critical ray in the case of a constant lapse rate and constant temperature, with the result:

$$x - x_o = 2\sqrt{\frac{Tz}{\gamma}} \qquad (4.8)$$

For a lapse rate of 6.5^o C/km, temperature of 273^o K and a mountain peak some 5 km above the mean terrain, any infrasound produced by the peak should be undetectable at distances beyond 30 km. This would correspond to the first zone of silence indicated in Fig. 4.2.

Thus it may be concluded that even though a mountain peak is producing infrasonic waves, they may be undetectable by a nearby receiving station.

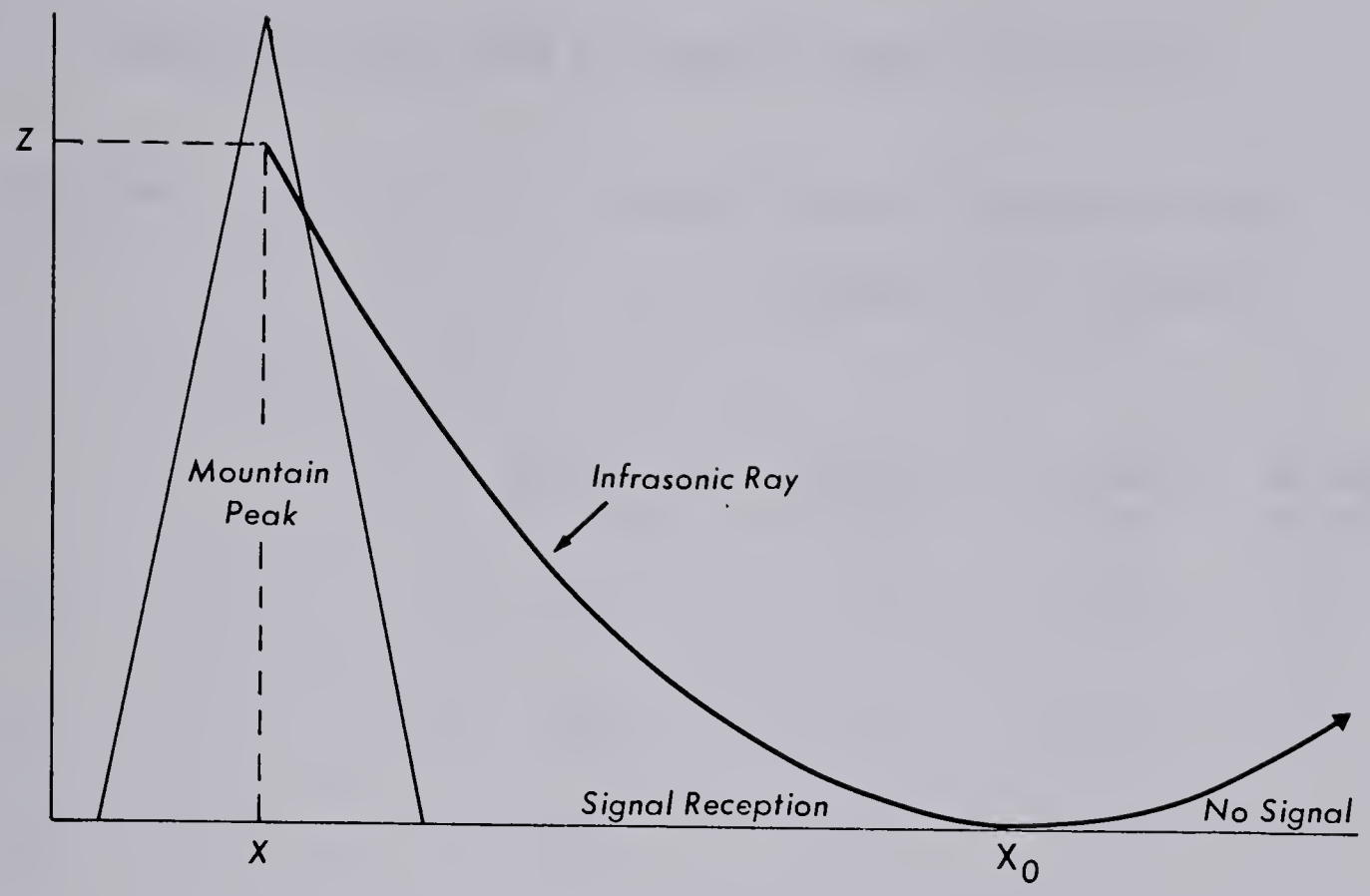

Fig. 4.4 Path of infrasonic ray produced by a natural dipole at height z

4.5 Wind Effects

Wind effects play an important role in determining the path of sound waves. Near the surface of the earth, where the wind speed is usually only a very small fraction of the speed of sound, such effects are rarely substantial. However, at the tropopause, in the vicinity of the jet stream at about 12 km, the wind speed can be as much as 25% of the sound speed. This causes dramatic changes in the course of a sound ray.

Table 4.1 gives a brief summary of the winds for the area over the continental United States.

TABLE 4.1

East-West Zonal Winds at Several Geometric Altitudes

Altitude km	Mean values of wind speed m/sec (+) - eastward, (-) - westward			
	16 Oct. to 31 March	1 April to 31 May	1 June to 15 Aug.	16 Aug. to 15 Oct.
50	+52	+2	-42	0
55	+58	-5	-47	+2
60	+61	-8	-51	+5

(Cook, 1969).

The mean north-south (meridional) wind speeds are less than 10 m/sec at any time of the year, and have an average value of 6 m/sec northward.

From Table 4.1, it is evident that at 50 km, in the winter months, the ground speed of an eastward propagating sound wave will be enhanced by 52 m/sec, while a westward propagating wave will be retarded by 52 m/sec (relative to the ground). The 50 km thick atmospheric layer between the stratopause and the surface of the earth serves as a waveguide for eastward propagation of sound waves during the winter months, but not for westward propagation. In summer the situation is reversed; the waveguide is effective only for westward propagation.

The component of the wind perpendicular to a sound wave will cause the wave to be deflected. This shift or azimuthal deviation is dependent on three factors (Rockway, 1972)*: the length of the propagation path, the magnitude of the wind, and the latitude of the final position of the ray. Rockway found that a wave travelling from 45^{o} N latitude to 55^{o} N latitude, and experiencing a 50 m/sec wind would have a 10 degree azimuthal deviation from a no-wind case. Obviously this could be important when trying to determine the origin of a sound wave.

---

* See Kimpo 1973.

Wind shear also has a significant effect upon the propagation direction of a sound wave. The normal situation in the atmosphere is one of increasing wind speed with height. Waves moving against the wind will be refracted upward, while waves moving in the direction of the wind will be refracted downward. (Fig. 4.5).

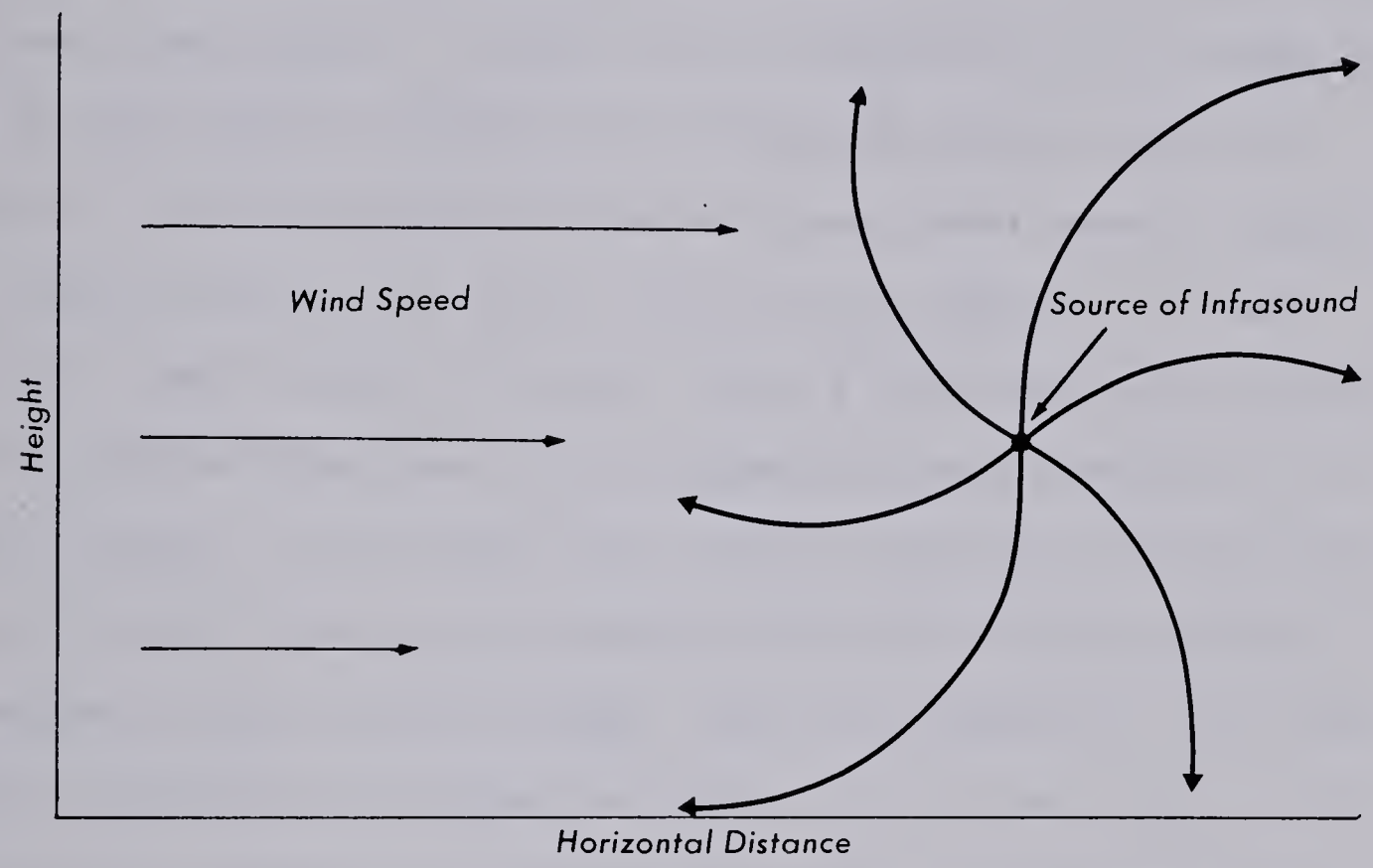

Fig. 4.5 Effect of vertical wind shear upon upwind and downwind propagation of sound waves.

The usual effect of wind shear is that the distance from the source in which infrasound can be detected is decreased, in the direction of the wind. A vertical wind shear of 6 m/sec/km is equivalent in refractive power to vertical temperature gradient of 10^{o} C/km.

4.6 Summary of Propagation Effects

The preceding sections show that a sound wave undergoes numerous changes enroute from source to receiver. Wind and temperature place the main role in determining the characteristics of the transmitted sound rays, while the attenuation of the infrasonic wave is negligible. Allowing for the effects of wind and temperature one might expect to predict the azimuth and elevation angle at which a sound wave would be received from a given source. However, a fairly detailed knowledge of the wind and temperature at each point along the way is required. Even if these data were available the precise computations of ray geometry would be difficult. But, as a general rule-of-thumb, ray azimuths should be shifted slightly to the east in the winter because of the effect of the prevailing westerly winds in mid-latitudes. Since the magnitude of this shift on a given day is not known, no corrections have been made in this study for azimuthal variations due to wind or temperature effects.

As a final thought, it should be noted that the azimuths from which the greatest percentage of sound waves are received may be strongly affected by the properties of the atmospheric waveguide which allows only certain preferred directions of propagation. Therefore a preferred azimuth range does not necessarily imply that the greatest number of sources are actually located within this range.

CHAPTER V

RECEPTION AND DIRECTION FINDING

5.1 Measurement and Recording

The system used to detect infrasonic signals at each of the stations is discussed by Cook (1969). A brief summary will be presented in this section.

An array of at least four microphones at each receiving station determines four characteristics of infrasonic waves passing through the area: 1) the amplitude and waveform of the incident sound pressure; 2) the horizontal phase velocity; 3) the distribution of sound wave energy at various frequencies, and; 4) the direction of propagation of the wave.

The microphones are located at ground level, approximately in the same plane, and about 7 km apart.

Effects of pressure fluctuations due to local turbulent eddies are minimized by a noise reducing system described by Daniels (1959), which consists of lines of pipe, having capillary inlets, and attached to the microphone.

The received signals are usually recorded on paper charts, one at each of the four microphone sites. The characteristics of the sound wave are then obtained by overlaying pairs of recordings from the four charts. This method requires an accurate timing trace

for each record and also assumes that the sound waves have approximately plane wavefronts.

5.2 Direction Finding

By overlaying the charts and visually correlating the waveforms from pairs of microphones the azimuth of the approach of the wave and the horizontal trace velocity can be obtained from a comparison of the time of arrival of the waveform at each microphone. Detection of signals is often difficult since local noise may obscure the desired signal, and superposition of signals arriving from two or more directions may cause the waveform to vary at each microphone.

Since it is often difficult to separate mountain-associated wave characteristics from outside influences, an "event" is assumed to occur when a narrow range of azimuths is observed for an extended period of time (usually greater than 2 hours). A variation in azimuth may be due to several factors. As mentioned, variation in waveforms at each microphone can cause poor correlations. Charts can be overlayed with an accuracy of $\pm$ 0.5 seconds for excellent signals. The quality of a signal is determined by the azimuth scatter obtained by overlaying pairs of charts. Excellent signals show a ½ to 1 degree scatter, while poor signals show a 6 to 10 degree scatter. Signals of greater scatter are ignored (Larson, 1971).

As noted in the previous chapter the path of a sound ray may be altered numerous times enroute from source to receiver.

The azimuth angle, in particular, varies according to the strength of the cross-wind component. Diamond (1963) has shown that the azimuthal error due to a cross-wind velocity can be estimated as:

$$\text{ERROR} = \tan^{-1} \frac{v}{c} \qquad (5.1)$$

where v = cross-wind velocity
c = speed of sound

Taking the possible direction-finding errors into account, Larson (1971) states "... azimuth angles for good signals do not have errors greater than 10 degrees."

5.2.1 Single Source

The most direct path of a sound ray is along the great circle route between a source and a receiver. If no distortions of the ray's path were present, there would be a single azimuth angle of arrival at a station. This is not the case, however. Instead a range of azimuths should be expected. If only one source is predicted by the dipole model, then there would be a 10 degree error in calculating the azimuth. In other words, a range of azimuths of $\pm$ 5 degrees around the true heading is the best that can be expected in most cases (Fig. 5.1).

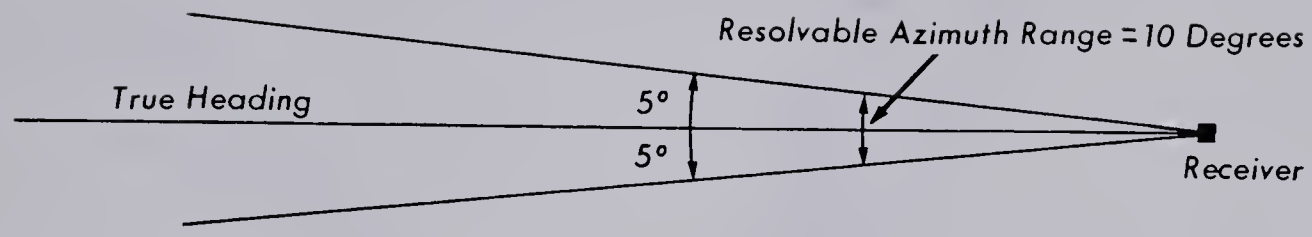

Fig. 5.1 Resolvable azimuth range around the true heading.

5.2.2 Two or More Sources

If the directions of two or more sources are to be determined by the dipole model, then an azimuth error of $\pm$ 5 degrees must be expected in each of the bearings of the respective sources. This means that the azimuths of the true headings of two sources must be at least 10 degrees apart for resolution between the two to be possible (Fig. 5.2).

In practice, however, direction finding must at times be somewhat subjective. For example, consider the situation in Fig. 5.3.

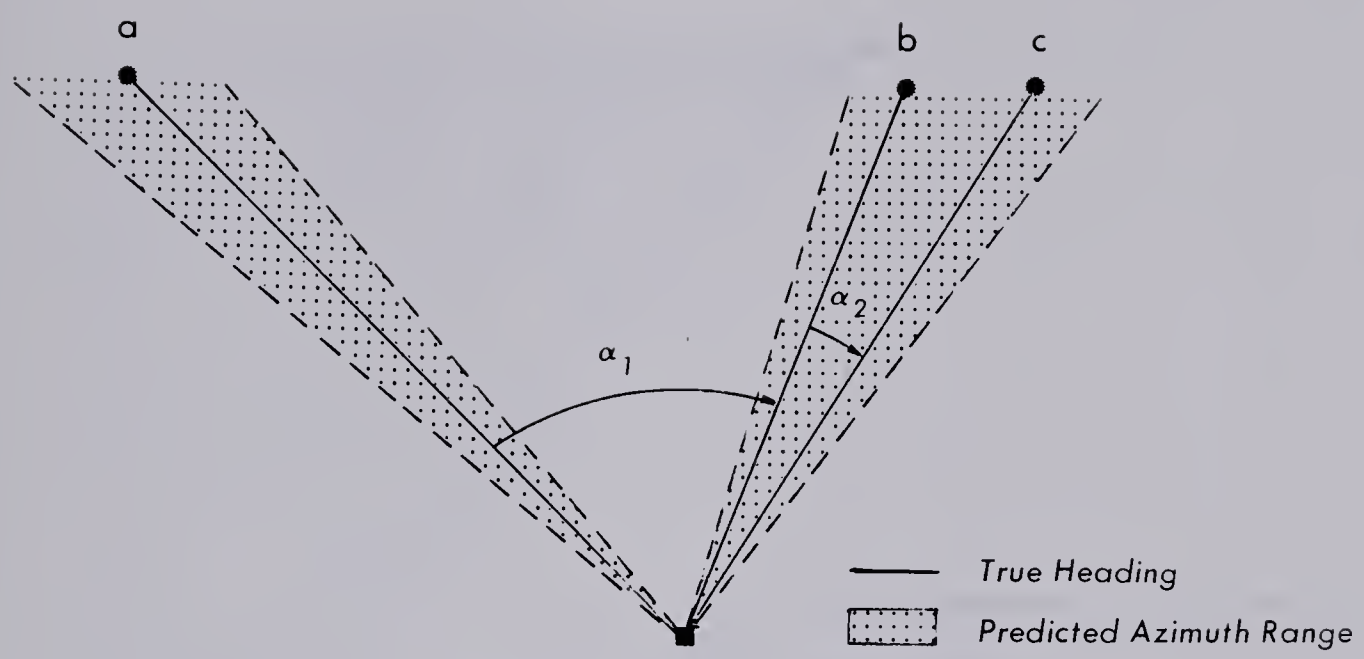

Fig. 5.2 Predicted azimuth ranges at a receiving station from three sources a, b, and c.

1. $\alpha_1 > 10^{\circ}$ - resolution between sources a and b (or c) is possible

2. $\alpha_2 < 10^{\circ}$ - resolution between sources b and c is not possible

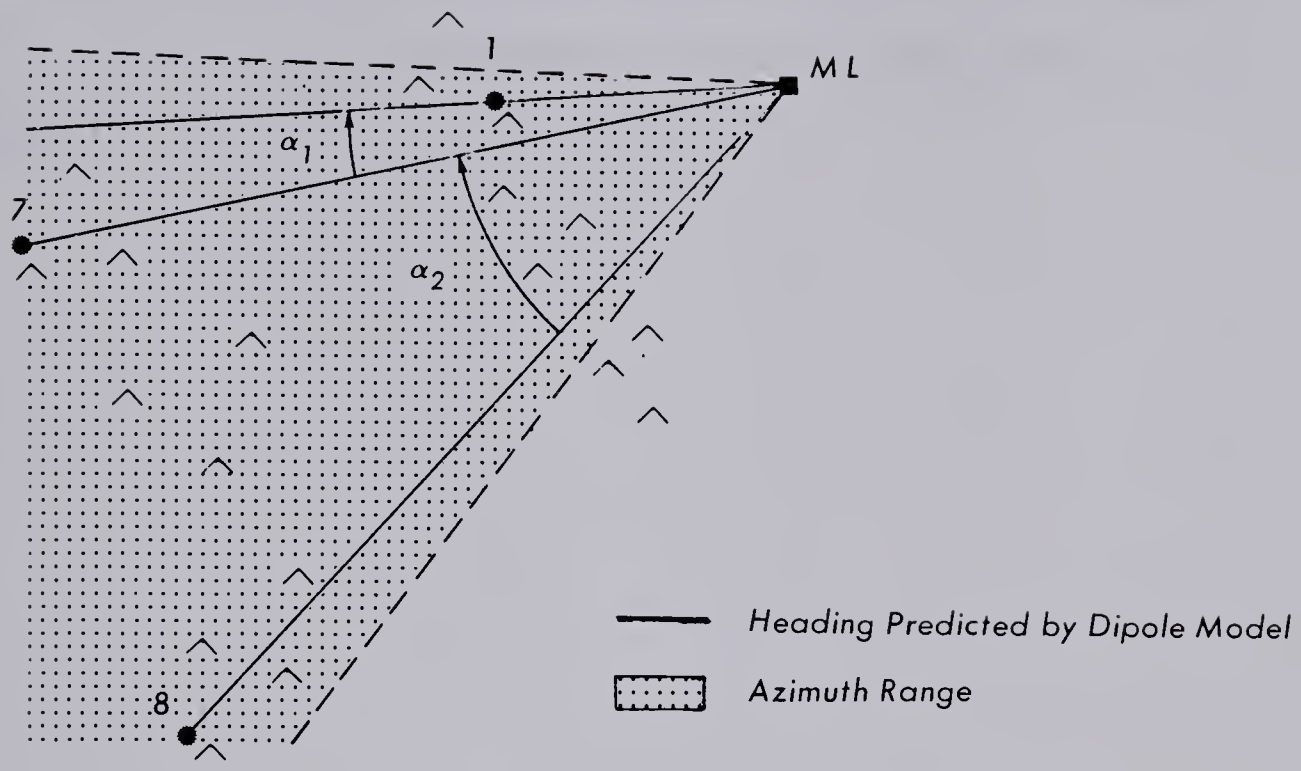

Fig. 5.3 Azimuth range for a receiver at Edson (ML) for sources at mountain locations 1,7 and 8

In this case the dipole model has predicted that a receiver at Edson, Alberta (ML) should receive three distinct signals; one signal from mountain location number 1, a second signal from location 7, and a third signal from location 8. The true bearings from sources 1 and 7 differ by only 8 degrees; thus it should not be possible to resolve signals produced by these two sources. On the other hand, since source 8 has a bearing differing by some 44 degrees from that of source 7, one could assume that these two sources may be easily distinguished. However, since the terrain

between the three sources is very mountainous, and all three locations are producing signals, one may suspect that signals may also be emitted by mountains in the region between sources 7 and 8. Thus, resolution between any of these three mountain locations appears to be very difficult. An azimuth range as shown in Fig. 5.3 is assumed.

CHAPTER VI

COMPARISON BETWEEN PREDICTED AND OBSERVED MOUNTAIN-ASSOCIATED WAVE CHARACTERISTICS

6.1 Infrasonic Triangulation Events

The first step in this analysis of infrasonic signals from unknown sources is the determination of probable triangulation events. A triangulation event is defined as an interval of time during which infrasonic signals are received at the triangulating stations. A natural requirement is that the stations receive signals at the appropriate relative times. Events are selected for study on the basis of the following criteria:

1) The events cover a relatively long interval of time, preferably greater than 2 hours. This improves the chances that a single dominant source is being observed.

2) The triangulation area is stable, ie. the azimuth angles are fairly steady throughout the observation interval; this again increases the chances that a single event or stable configuration of events is being detected.

3) Meteorological data must be available for the time during which the event was recorded.

Four stations were involved in the detection of infrasonic signals and the subsequent determination of triangulation points:

1. Fairbanks (or College), Alaska: 64.51°N, 147.43°W
2. Pullman-Washington, Washington: 46.44°N, 117.10°W
3. Boulder, Colorado : 40.01°N, 105.17°W
4. Edson, Alberta : 53.35°N, 116.26°W

(Edson was a temporary station taken out of service in 1973.)

Following the format adopted by other authors, the following abbreviations will be employed for convenience:

Edson - ML Pullman - PW

Fairbanks - CO Boulder - BO

(See Fig. 6.1)

In order to locate a triangulation area, a signal must be received by at least two of these stations at the proper relative times.

The location and times of the triangulation areas which were chosen for study are given in Table 6.1 (also Fig. 6.1).

TABLE 6.1

Infrasonic Triangulation Events for Aug. 1971 to Feb. 1972

EVENT	DATE	TIME (Greenwich Mean)	LATITUDE (Degrees North)	LONGITUDE (Degrees West)
1	30/09/71	0030-0800	55	126
2	05/10/71	0000-0100	53	125
3	07/10/71	2130-2300	46	122
4 a)	08/10/71	0000-1130	56	125
b)	08/10/71	2300-2400	60	130
c)	09/10/71	0000-0130	59	129
5	18/11/71	0800-1600	57	128
6	01/12/71	0400-0600	60	155
7	29/12/71	0030-0200	57	130
8	14/01/72	0030-0230	46	114
9	18/01/72	0730-1330	41	110
10	25/01/72	0200-2300	51	125
11	26/01/72	0000-2400	54	122
12	27/01/72	0000-0500	54	123
13	01/02/72	0030 0930	60	120
14	02/02/72	0030-0530	57	125
15	03/02/72	0030-0430	56	120
16	09/02/72	0730-1200	58	127

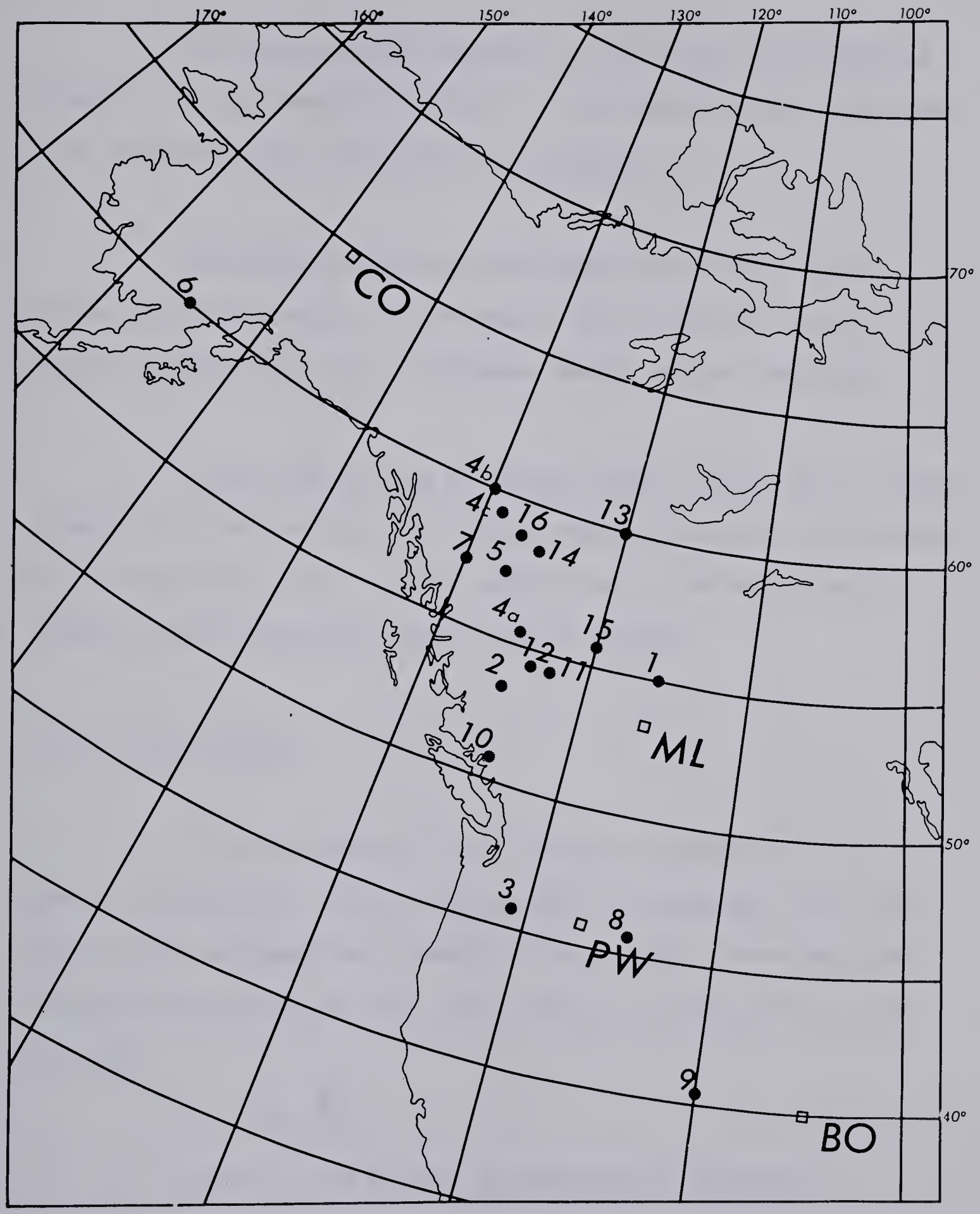

Fig. 6.1 Infrasonic triangulation events for Aug. 1971 to Feb. 1972.

6.2 Meteorological Data

The dipole model requires, as input, the wind speed and direction at each mountain location. It is also desirable that these data be observed near the peak of the mountain.

The data are obtained from upper level charts which contain such information as wind speed, wind direction, contour height, temperature, etc. at different levels in the atmosphere.

Since measurements are rarely taken directly at a mountain location, the wind velocity at the ten source sites must be estimated using neighboring data. A brief explanation of the method used to obtain the wind velocity at each location follows.

6.2.1 Wind Velocity

The measurement of wind velocity is needed near the peak of the mountain. The available upper-air maps were the 700-mb charts which correspond to a height of about 3000 m above sea level. In order to estimate the wind speed, the geostrophic wind equation is used:

$$V_g = \frac{g}{f} \frac{\delta Z}{\delta H} \qquad (6.1)$$

where $f = 2\,\Omega \sin\phi$ is the Coriolis parameter

and V_g = geostrophic wind

g = gravitational acceleration (9.81 m/sec^2)

Ω = Earth's angular velocity (0.729×10^{-4}/sec)

ϕ = latitude at which the geostrophic wind is to be calculated

δZ = standard contour interval (60 gpm or approx. 60 m)

δH = horizontal spacing of contour lines

Using a latitude of $\phi = 50^{o}$ N gives a value for the geostrophic wind as:

$$V_g = 5.23 \times 10^6 / \delta H \qquad (6.2)$$

from which V_g merely becomes a function of the spacing of the contour lines.

The primary assumptions underlying Equation 6.1 are that the frictional force and the acceleration are small in comparison to the pressure and Coriolis forces. A strict balance between pressure and Coriolis forces is thus implied which is true only if the contour lines are straight and parallel. Since most contours are curved, an error of up to 10% may be introduced. Also, the Coriolis parameter varies with latitude. However, the error produced by assuming no variation is negligible in mid-latitude. The geostrophic equation also ignores terrain effects by assuming that the frictional forces are small. At low altitudes this would be a serious source of error; however, at 700-mb the frictional forces are very small and can usually be ignored. The geostrophic wind Equation (6.1) will, in most cases, provide an overestimate of the actual wind speed.

The wind speed at the various mountain peaks can be obtained merely by measuring the spacing between the contour lines and applying Equation 6.2. The wind direction is also easily obtainable since the geostrophic assumption implies that it be parallel to the contour lines.

In practice it may not be necessary to use Equation 6.2 to estimate the wind speed. By taking note of the speed at neighboring stations a good estimate can often be made at the source location.

6.3 Computational Prccedure

The intensity of the dipole radiation is given by Equation 3.1. For the accuracy attainable in the calculation of the intensities it is sufficient to assume a constant temperature of $-15^{o}C$ (258^{o} K) at 700-mb over the period in which the infrasonic events were recorded (August to February). The air density and sound velocity (which are functions of temperature) will have the values:

$$\rho = 1.3 \text{ kg/m}^3$$

$$c = 320 \text{ m/sec}$$

The kinematic viscosity of air is 1.2×10^{-5} m^2/sec and the average peak diameter was estimated to be 500 m. Inserting these values into Equation 3.1 gives:

$$I = 109 \frac{U^7 y^2}{r^2} \sin^2\theta \qquad (6.3)$$

Using a 700-mb upper-air chart corresponding to the period of observation of an infrasonic event, the following procedure is performed for each of the ten source locations:

1) Estimate the wind speed, U.

2) Calculate the angle, θ , for each station.

3) Obtain the peak height, y, and distance to station, r (Table 6.2).

4) Use the above values for U, θ , y, and r to predict the dipole intensity at each of the four stations.

Once the intensities from each source at a given station are calculated they are ranked according to order of magnitude. This serves to separate the dominant source, or sources, for each station. The dominant source is assumed to have an intensity of one or more orders of magnitude greater than the remaining sources.

From this information a range of azimuths at each station is predicted as outlined in Chapter V. The intersection of the azimuths from two or more of the receiving stations defines a triangulation region. This region can then be compared to the observed triangulation point for the infrasonic event under study.

TABLE 6.2

Peak Heights and Distances From Receivers to Sources

Mountain Location	Peak Height, y (m)	Distance to Receiver, r (km)			
		ML	CO	PW	BO
1	1454	186	2049	741	1783
2	446	729	1411	1378	2427
3	472	1410	806	2082	3111
4	261	2247	521	2918	3945
5	3694	2262	243	2792	3933
6	3550	1657	569	2176	3318
7	1542	648	1957	793	1980
8	1892	845	2544	334	1499
9	1918	1895	3681	1125	1205
10	1399	1759	3874	1203	141

6.4 Results

The results are interpreted mainly on the degree of proximity between the predicted region and the observed triangulation point. In this way a subjective judgement is made as to the likelihood of a dipole being the source for the observed MAW event.

The results of the dipole model are given in Appendix A.

Since $I \propto U^7$ in the dipole model, the predicted triangulation region could be expected to be in the areas of maximum wind speed ie. the jet stream. This was indeed true in the majority of cases. A plot of the latitude of the observed MAW event versus the latitude of the 500-mb jet stream is shown in Fig. 6.2. The correlation between the two suggests that the wind speed may be a major factor in the production of MAW.

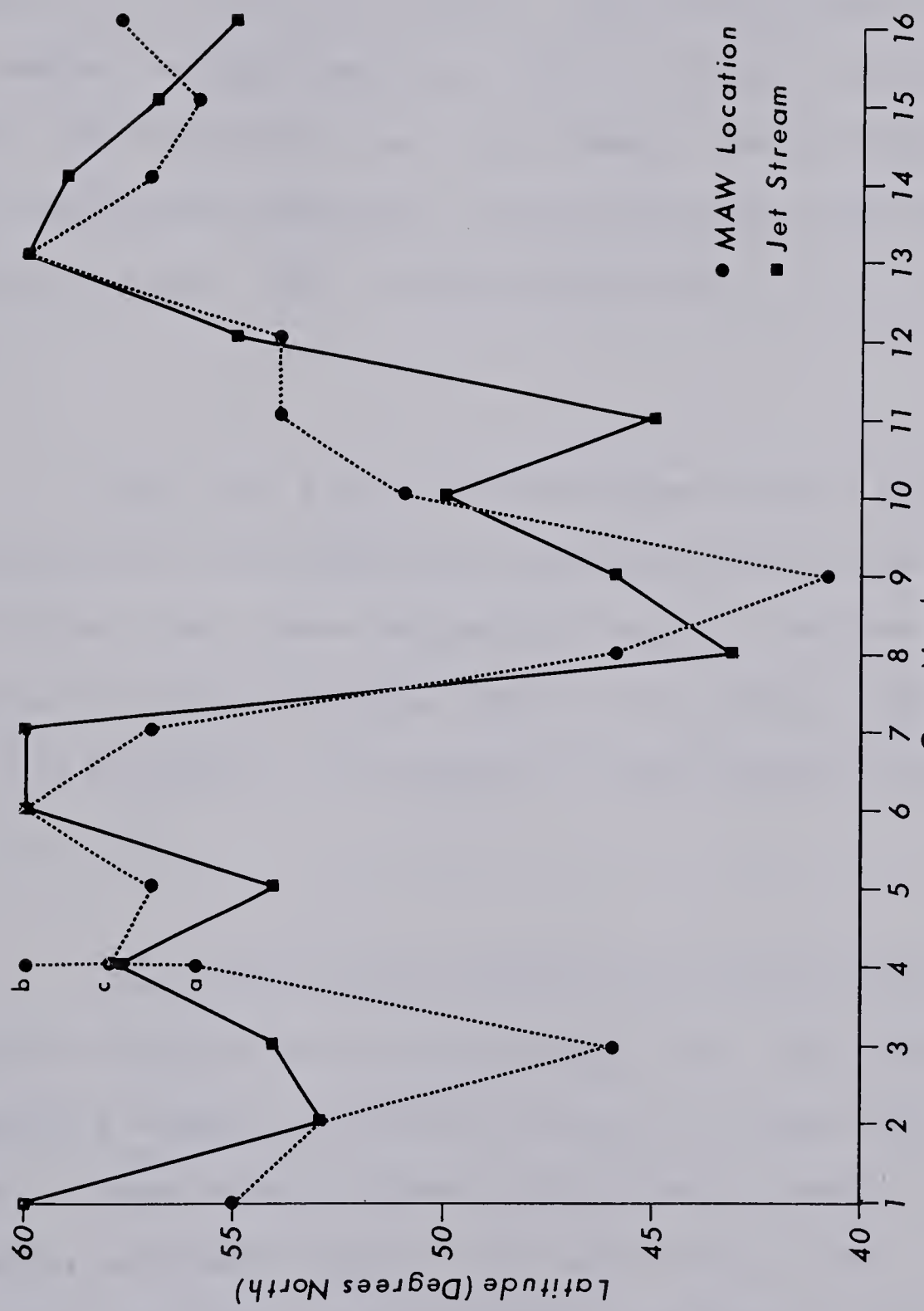

Fig. 6.2 Latitude of MAW Event and Jet Stream for each of the 16 cases

Examination of the results from the dipole model contained in Appendix A indicates that when closely spaced contour gradients (ie. strong winds) were present over the mountains, both the predicted triangulation area and the observed source point were usually located in the region of maximum wind. This is particularly evident in cases 2, 4, 5, 7, 8, 9, 15, and 16. Under the influence of a tight gradient the predicted areas tended to follow a fairly organized pattern. When the gradient was slack, however, the predicted regions were ill-defined and showed very little correlation to the observed triangulation point. This is evident from cases 1, 11, 12, 13, and 14.

Cases 3 and 5 show a well-developed gradient across the mountains, but the observed and predicted regions do not coincide. In particular, Case 3 shows the predicted region in southern Alaska, an area with strong upper winds. However, the observed triangulation point is in Washington, in the center of a high pressure area with only light winds.

Case 5 occurred while strong winds prevailed over much of southern Alaska and the British Columbia coast. The predicted triangulation regions coincide with the zone of maximum winds. The existence of three separate areas is most likely a result of subdividing the mountainous regions into three distinct source locations. It is thus likely that the dipole model could predict a region extending along the coast from southern British Columbia to the Gulf of Alaska. This could mean that, though the observed point falls within the boundary of this predicted region, there is such great

uncertainty in the precise location of the predicted area that it would be difficult to deduce any useful correlations.

Case 6 also shows the actual triangulation point to be well-removed from the axis of maximum wind. The dipole model does predict a source at the observed point; however, the major source is located in the tight gradient area well to the south.

Case 4 is particularly interesting in that it involves three distinct triangulation points located in a tight contour gradient area. The predicted region is also within this tight gradient and actually encompasses two of the three points, the third being only slightly outside this area.

Additional testing of the model was done by considering cumulative statistics for the 16 cases. The predicted arrival azimuths from which signals are received for each station are shown in Fig. 6.3 through 6.6. The predominant signal emitters for the receiver at Edson are observed at an azimuth of 260 degrees. There are three lesser azimuths of 308, 252 and 208 degrees (Fig. 6.3). This may be compared to Fig. 1.1 which shows the majority of signals arriving from about 300 degrees. The College data predict the major azimuth at 138 degrees (Fig. 6.4). The Pullman-Moscow observatory has forecast azimuths of 273 degrees and 324 degrees (Fig. 6.5). Boulder shows a preferred azimuth at 222 degrees and another lesser heading from 325 degrees (Fig. 6.6).

Since observed arrival azimuth statistics are available only for the Edson receiver, no comparison was made between predicted and observed results for the other three receivers.

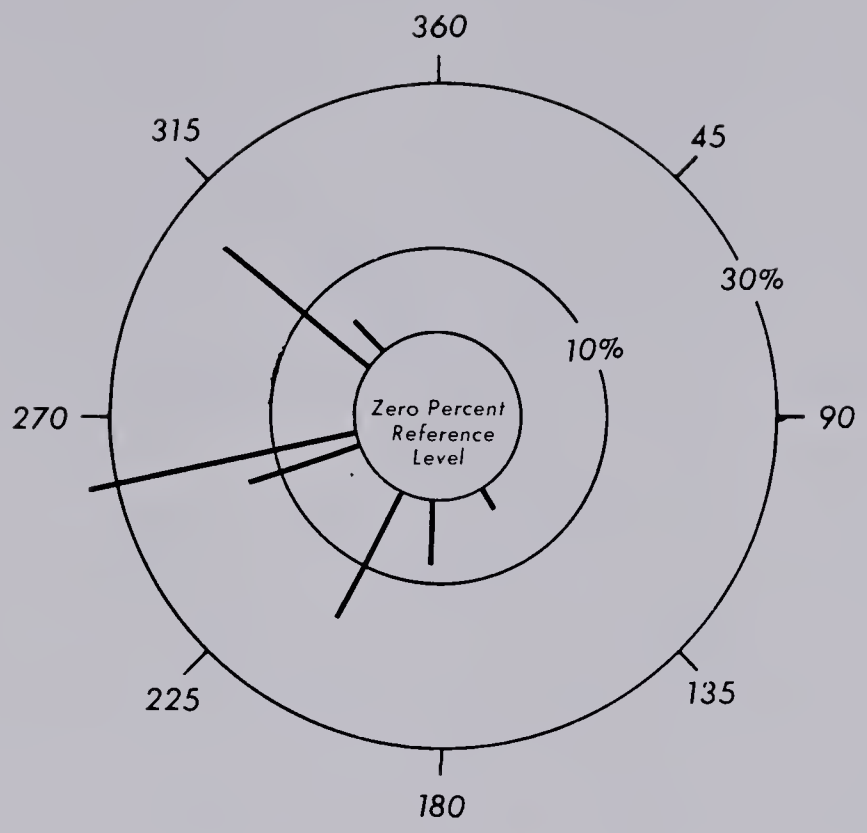

Fig. 6.3 Percentage of signals received along predicted arrival azimuths at Edson, Alberta

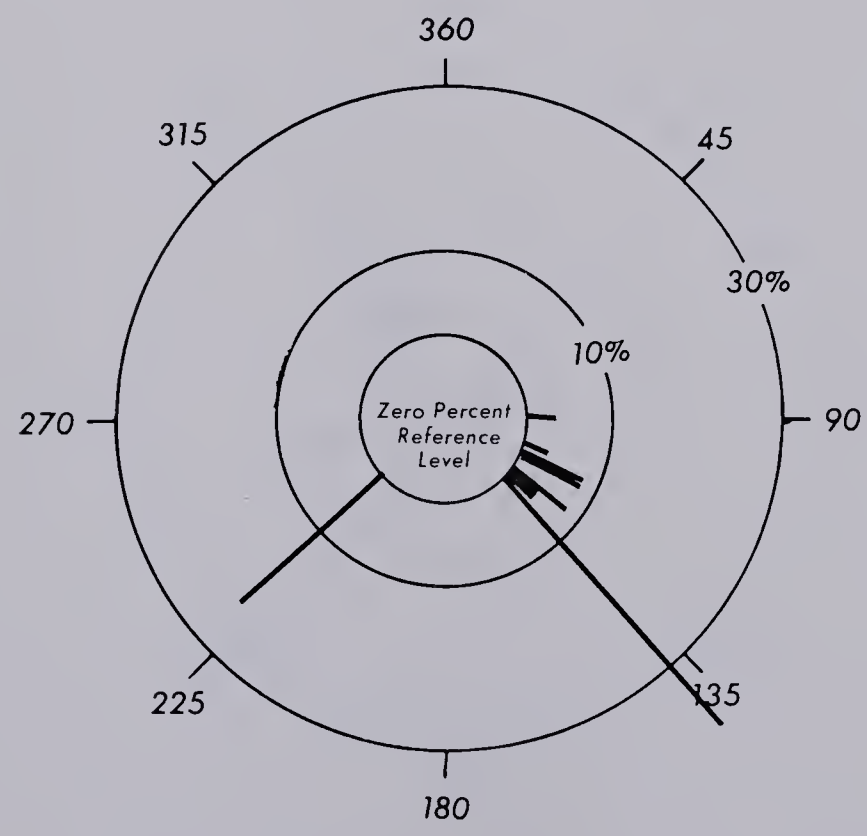

Fig. 6.4 Percentage of signals received along predicted arrival azimuths at College, Alaska

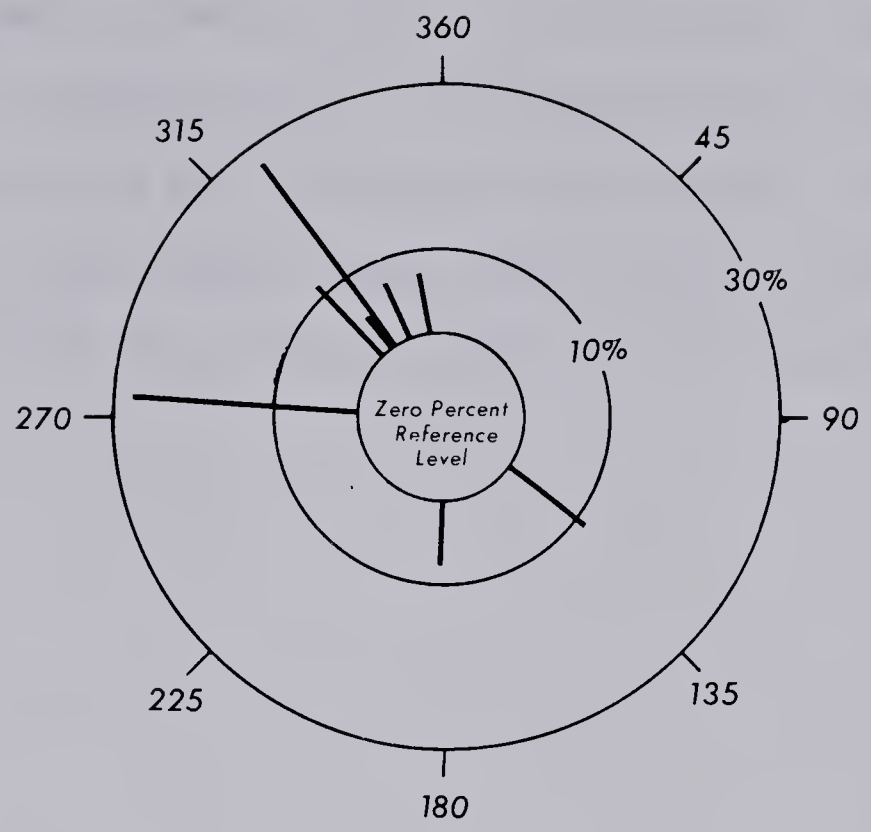

Fig. 6.5 Percentage of signals received along predicted arrival azimuths at Pullman-Moscow, Washington

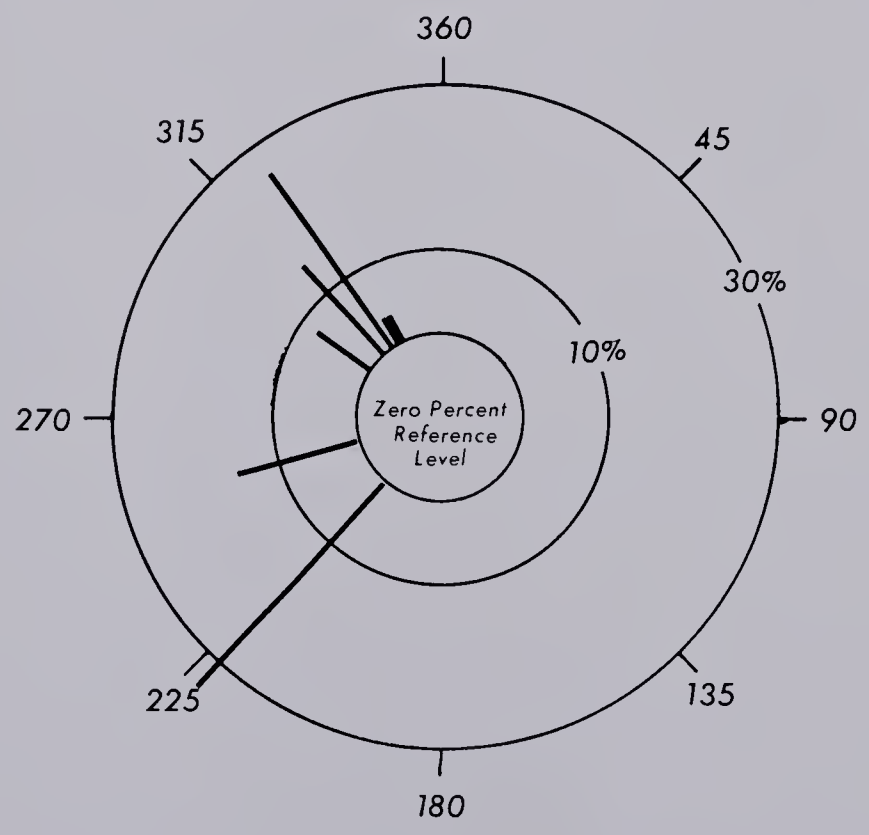

Fig. 6.6 Percentage of signals received along predicted arrival azimuths at Boulder, Colorado

It is customary to measure the power of a signal rather that the intensity. According to Larsen (1971) the observed pressure amplitudes for MAW vary from 0.5 μb to about 7.5 μb zero-to-peak (as compared to typical atmospheric pressures of 1000 mb). However, no comparisons have been made between observed and theoretical sound pressures in the present study, since the simple model does not take into account the effects of attenuation and anomalous propagation.

CHAPTER VII

SUMMARY AND CONCLUSIONS

Theoretical and experimental findings have shown that the flow of air around a stationary cylinder will result in the conversion of kinetic to acoustical energy for sufficiently large Reynolds numbers. The sound produced in this manner is termed aerodynamic sound in that it is not a result of vibrations of the cylinder itself, but rather accompanies the shedding of vortices in the wake of the cylinder. The associated sound field possesses a dipole pattern with the main axis perpendicular to the flow.

By enlarging the concept of a flow of air past a cylinder to an analogous flow of air past a prominent mountain peak a model for the generation of Mountain-Associated-Infrasonic-Waves has been developed. The observation of Kármán vortex streets in the lee of mountain peaks added further support for the theory of a natural dipole generator.

In Chapter V the propagation of infrasound through the atmosphere was examined. It is evident that the path of a sound wave may vary greatly due to changes in the state of the atmosphere. Since ray-tracing theory requires a detailed knowledge of winds and temperature, it was considered beyond the scope of this study to correct propagation paths by allowing for the effects of varying wind and temperature conditions. The main conclusion reached is

that the largest percentage of sources may not actually lie within a preferred range of azimuths, since propagation effects may determine the direction from which signals can be detected.

Moreover, sensing and recording of infrasonic signals includes errors which make direction finding difficult; hence, a range of azimuths should be expected rather than a single heading. In most cases the intersection of azimuthal ranges from two or more of the receiving stations defined a triangulation region.

Wind data corresponding to the times of observed MAW events were used in the model to predict signal source regions. The results were judged according to the proximity of the observed and predicted areas.

In 9 out of 16 cases examined (case numbers 2, 4, 5, 6, 7, 8, 9, 15, 16) it appears that a dipole oscillator could be responsible for the production of the observed MAW events. However, one cannot assume that it is the only mechanism generating the observed signal. When a well-developed contour gradient exists across the mountains, the dipole model predicts regions which are in fairly close proximity to the observed points, but when the flow is weak the predictive skill of the model is low.

It is important to keep in mind that the input for the model comes from data collected at one specific time of the day, whereas a MAW event may occur over a period of several hours.

Changing wind conditions during the day may cause a corresponding change in forecast triangulation areas. It may be that the upper-air data, reported at 0000 Z and 1200 Z, do not adequately represent the wind pattern prevailing during the time of the recorded MAW event.

The 700-mb upper-air chart was used to obtain wind data. This chart corresponds to an altitude of approximately 3000 M above sea level. The highest peaks, such as Mt. Robson, Mt. Fairweather and Mt. Logan, range from about 4000 to over 6000 m above sea level, well above the 700-mb level. The wind conditions will normally be different at the level of these peaks because, in most instances, the wind speed increases with height. If calculations for the higher peaks are based only on 700-mb winds, then the sound intensity would be expected to be too low. Since $I \propto U^7$, the intensity should increase with height. The higher peaks may thus be still dominant dipole sources and the resultant triangulation region need not be affected to any great extent. The direction of the wind has only a slight effect on the intensity of infrasound produced by the dipole model, unless the wind vector is very nearly parallel to the radius vector from the source to the receiver. Thus, even if the direction of the wind changes with height, this effect will most likely be overshadowed by a change in the speed of the wind.

Observation shows that the majority of the signals received at Edson, Alberta arrive from about 300 degrees (Fig. 1.1). The predicted azimuths of arrival for Edson (Fig. 6.3) do show that

a large percentage of signals could be expected to come from this heading; however, the majority come from about 260 degrees. The source producing these signals is most likely Mt. Robson, which is only some 180 km from the Edson receiving array. As outlined in Chapter IV on propagation, a receiver situated 100 to 200 km from a source may be unable to detect signals. If this were the case with Edson and Mt. Robson, then a number of signals coming from the direction of 260 degrees may be undetectable, meaning the largest percentage of signals would arrive from about 310 degrees.

From a sample of only 16 cases it is difficult to draw any definite conclusions concerning the degree to which the dipole model accounts for the observed MAW events. Results from the model show good agreement with observations in a number of cases, suggesting that dipole oscillators may generate Mountain-Associated-Waves under high wind conditions. Other mechanisms for the production of infrasound are likely contributing as well. "Natural" quadrupoles, formed in the turbulent flow over the mountains as well as in clear-air-turbulence, may also be important sources of infrasonic signals.

To date, little experimental work has been carried out at very high Reynolds numbers ($> 10^8$) corresponding to atmospheric flow around obstacles the size of mountains. It may be that the function, f(R), used in calculating intensities is different, at such high Reynolds numbers, from experimental results obtained in the laboratory.

Since Mountain-Associated-Waves are a fairly recent discovery, more data are needed before any definite conclusions can be drawn as to their origin and production mechanism.

REFERENCES

Bates, A.E. and R.B. Stephens, 1966: Acoustics and Vibrational Physics. Edward Arnold Ltd., London. Chapter 15.

Bayliss, P., 1976: Weather, 31, 346.

Bowman, G.G., S. Howard and A.J. Bedard, 1971: Observations of Infrasound Subsonic and Disturbances Related to Severe Weather. Geophys. J.R. Astron. Soc. 26, 215-242.

Campbell, W.H. and J.M. Young, 1963: Auroral-Zone Observance of Infrasonic Waves Related to Ionospheric Disturbances and Geomagnetic Activity. J. Geophys. Res., 68, 5909-5916.

Cook, R.K., 1969: Atmospheric Sound Propagation. Atmospheric Exploration by Remote Probes, National Academy of Sciences Panel on Remote Atmospheric Probing, 2, 633-669.

Cook, R.K., 1962: Strange Sounds in the Atmosphere. Sound 1(2), 12-16.

Craine, L.B. and J.E. Thomas, 1970a: Infrasonic Waves Observed from Mountainous Regions. Paper delivered at annual meeting of Am. Geophys. Union, Washington, D.C. (April, 1970).

Craine, L.B. and J.E. Thomas, 1970b: Infrasonic Waves in the Pacific Northwest. Continued proposal resulting in National Science Foundation Grants GA-23176 and GA-23203 (June, 1970).

Curle, N., 1955: The influence of Solid Boundaries upon Aerodynamic Sound. Proc. Roy. Soc. London, A 231, 505-514.

Daniels, F.B., 1959: Noise-Reducing Line Microphone for Frequencies Below 1 cps. J. Acoust. Soc. Am., 31, 529-531.

Diamond, M., 1963: Cross-Wind Effect on Sound Propagation. J. Appl. Meteorol., 3, 208-210.

Donn, W.L. and M. Ewing, 1962: Atmospheric Waves from Nuclear Explosions-Part II, The Soviet Test of October 30, 1961. J. Atmos. Sci., 19, 264-273.

Etkin, B., G.K. Korbacher and R.T. Keefe, 1957: Acoustic Radiation from a Stationary Cylinder in a Fluid Stream. J. Acoust. Soc. Am., 29, 30-36.

Fehr, U., 1967: Measurements of Infrasound from Artificial and Natural Sources. J. Geophys. Res., 72, 2403-2417.

Fleagle, R.G. and J.A. Businger, 1963: An Introduction to Atmospheric Physics. Academic Press, New York. Chapter 7.

Gaster, M., 1969: Vortex Shedding from Slender Cones at Low Reynolds Number. J. Fluid Mech., 38, 565-576.

Gazaryan, Y.L., 1961: Infrasonic Normal Modes in the Atmosphere. Soviet Physics-Acoustics, 7, 17-22.

Gerrard, J.H., 1963: The calculation of the Fluctuating Lift on a Circular Cylinder and its Application to the Determination of Aeolian Tone Intensity. Advisory Group for Aeronautical Res. and Dev. (AGARD), Report 463.

Gerrard, J.H., 1955: Measurements of the Sound from Circular Cylinders in an Air Stream. Proc. Phys. Soc. London, 68, 453-461.

Goerke, V.H. and M.W. Woodward, 1966: Infrasonic Observation of a Severe Weather System. Monthly Weather Review, 94, 395-398.

Goerke, V.H., J.M. Young and R.K. Cook, 1965: Infrasonic observations of the May 16, 1963 Volcanic Explosion on the Island of Bali. J. Geophys. Rev., 70(24), 6017-6022.

Gossard, E.E. and W.H. Hooke, 1976: Waves in the Atmosphere. Scientific Publishing Co., New York. Chapter 9.

Greene, G.E. and J. Howard, 1975: Natural Infrasound: A One Year Global Study.

Holle, Von W., 1938: Akust. Z., 3, 321.

Humphreys, W.J., 1964: Physics of the Air. Dover Publications, New York, Chapters 2 and 3.

Kimpo, F.L., 1973: Natural Aerodynamic Sound as a Source of Mountain-Associated-Infrasonic Waves. Master's Thesis, Dept. of Electrical Engineering, Washington State University.

Larsen, R.J., 1971: Correlation of Wind and Geographical Features with the Production of Certain Infrasonic Signals in the Atmosphere. Geophys. J. Roy. Astron. Soc., 26, 201-214.

Lighthill, M.J., 1962: On Sound Generated Aerodynamically. Proc. Roy. Soc. London, A267, 147-182.

Lighthill, M.J., 1952: On Sound Generated Aerodynamically, I, General Theory. Proc. Roy. Soc. London, A211, 564-587.

Lighthill, M.J., 1954: On Sound Generated Aerodynamically, II, Turbulence as a Source of Sound. Proc. Roy. Soc. London, A222, 1-32.

Maeda, K. and J. Young, 1966: Propagation of Pressure Waves Produced by Aurora. J. Geomagn. Geoelectr., Kyoto, 18, 275-299.

Meecham, W.C., 1971b: On Aerodynamic Infrasound. J. Atmos. Terres. Phys., 33, 149-155.

NASA, 1967: Earth Photographs from Geminii III, IV, and V, 123.

Perkeris, C.L., 1948: The Propagation of a Pressure Pulse in the Atmosphere. Phys. Rev., 73, 145-154.

Phillips, O.M., 1956: The Intensity of Aeolian Tones. J. Fluid Mech. 1, 607-624.

Rand McNally, 1969: The International Atlas, Rand McNally and Co., New York, 166-173.

Roshko, A., 1953: On the Development of Turbulent Wakes From Vortex Streets. National Advisory Committee on Aeronautics (NACA). Tech. Note 2913, 1-77.

Roshko, A., 1954a: On the Development of Turbulent Wakes from Vortex Streets. NACA report 1191, 1-20.

Roshko, A., 1954b: On the Drag and Shedding Frequency of Two-Dimensional Bluff Bodies. NACA Tech. Note 3169, 1-29.

Roshko, A., 1961: Experiments on the Flow Past a Circular Cylinder at Very High Reynolds Number. J. Fluid Mech., 10, 345-356.

Strouhal, V., 1878: V. Wied. Ann., 5, 216.

Teunissen, H.W., 1977: Global Flow-Visualization. Atmosphere, 15, 54-56.

Thomas, J.E. and L.B. Craine, 1971: Acoustic Gravity Wave Propagation in a Measured Atmosphere. Paper submitted for publication to Geophys. J. Roy. Astron. Soc.

World Meteorological Organization, 1967: The Airflow over Mountains. WMO Tech. Note #34, Geneva, Switz., 1-133.

APPENDIX A

PREDICTED TRIANGULATION REGIONS

This appendix contains the results obtained from the dipole model. The shaded areas indicate the predicted triangulation region for the production of Mountain-Associated-Waves. The observed triangulation points are indicated by stars.

Immediately following is an example of the method used to predict the triangulation region. Case 2 is selected since it is reasonably straight forward. Table A1 contains the intensities expected at the receivers from each of the mountain locations as obtained from the model, by use of Eqn. 6.3. The Edson (ML) receiver shows two dominant sources in mountain locations 1 and 7 (ie. Mt. Robson and Mt. Waddington respectively). The College (CO) receiver has dominant sources in mountain locations 6 and 7 (Mt. Logan and Mt. Waddington respectively); Pullman (PW) has dominant sources in locations 1 and 7; Boulder (BO) has a dominant source in location 7 only. Using Edson as an example, a line is drawn from Source 1 to the receiver at Edson (Fig. A1). Using direction finding methods, an azimuth range is assumed. The same is done for Source 7 to Edson. In this way a complete azimuth range is constructed for infrasonic signals arriving at the receiver at Edson. The same procedure is followed at each of the remaining three stations. Finally a triangulation region is defined by the intersection of azimuth ranges from each receiver (shown as the

shaded area in Fig. A1).

For the sake of clarity only the predicted triangulation region is shown for the remaining cases.

TABLE A1

Predicted Intensities at receiving stations

(in units of nt m^{-1} sec^{-1} x 10^{-2})

Mountain Location	Station			
	ML	CO	PW	BO
1	*6160	29	*529	30
2	2	1	4	0
3	0	0	0	0
4	0	0	0	0
5	0	3	0	0
6	51	*115	15	9
7	*1030	*941	*3810	*430
8	0	0	2	0
9	2	0	5	0
10	0	0	0	0

* - most likely source from which signals would be received

Fig. A1 Method used to construct the predicted triangulation area.

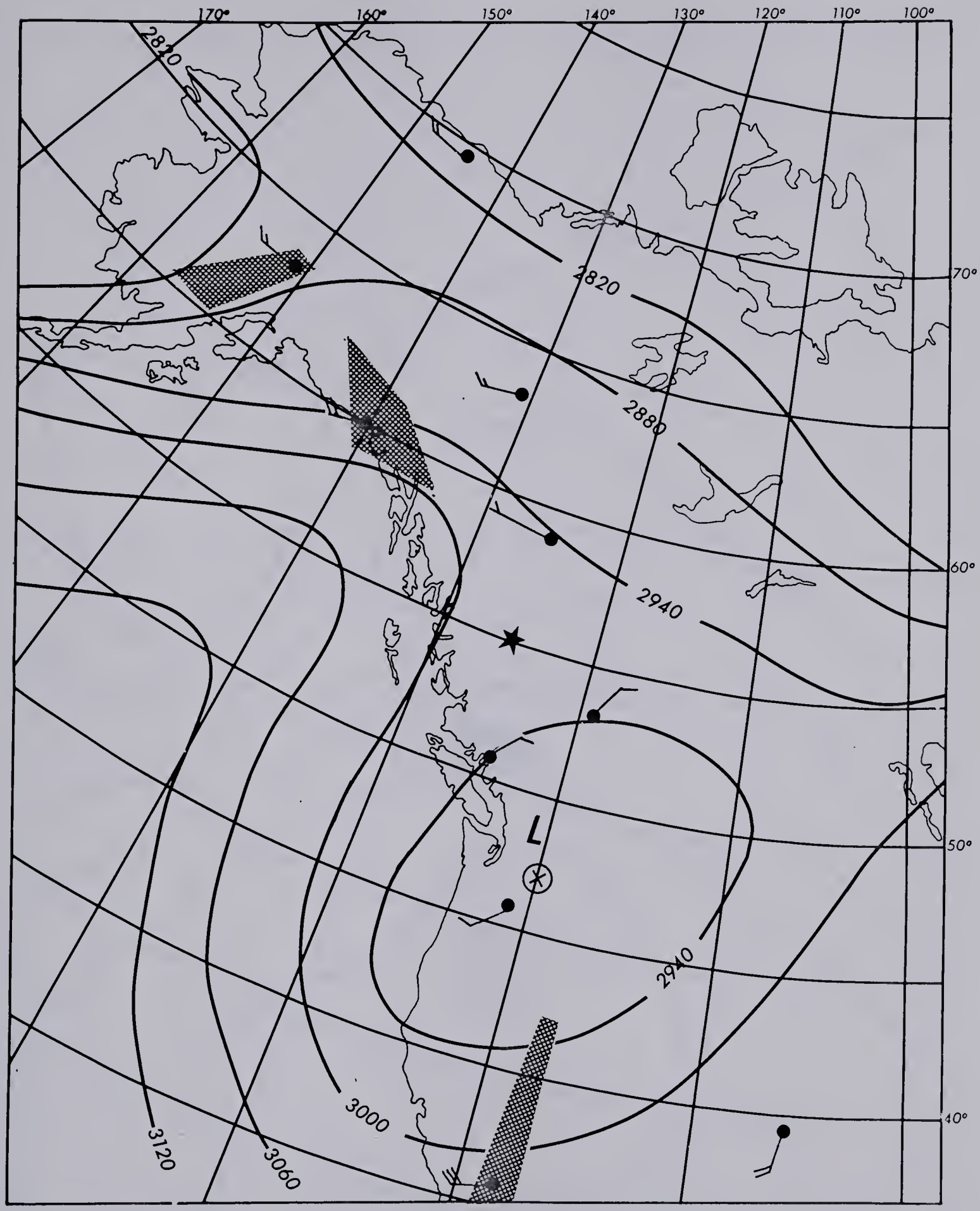

Case 1 700 mb 00Z 30 Sep 71

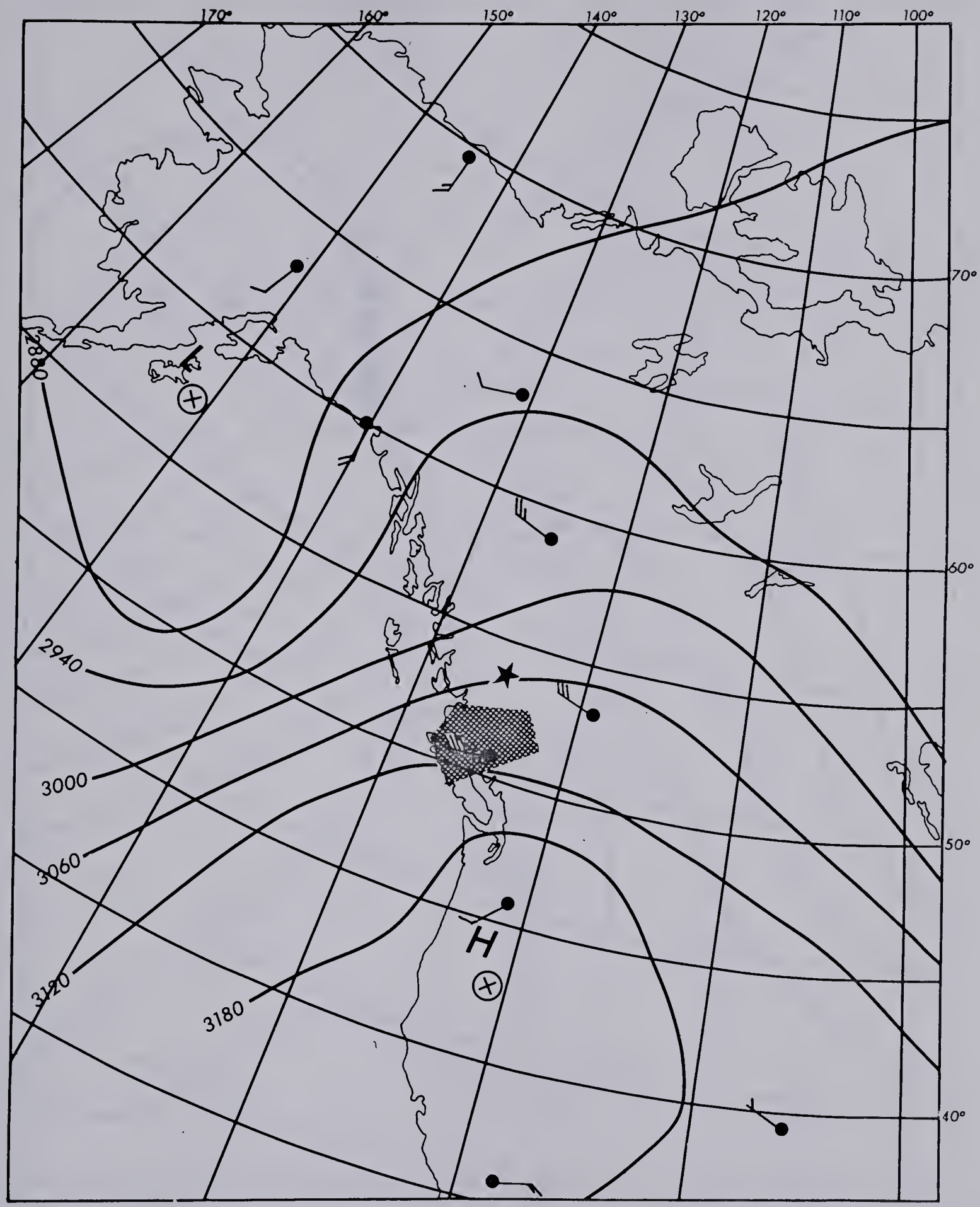

Case 2 700 mb 00Z 05 Oct 71

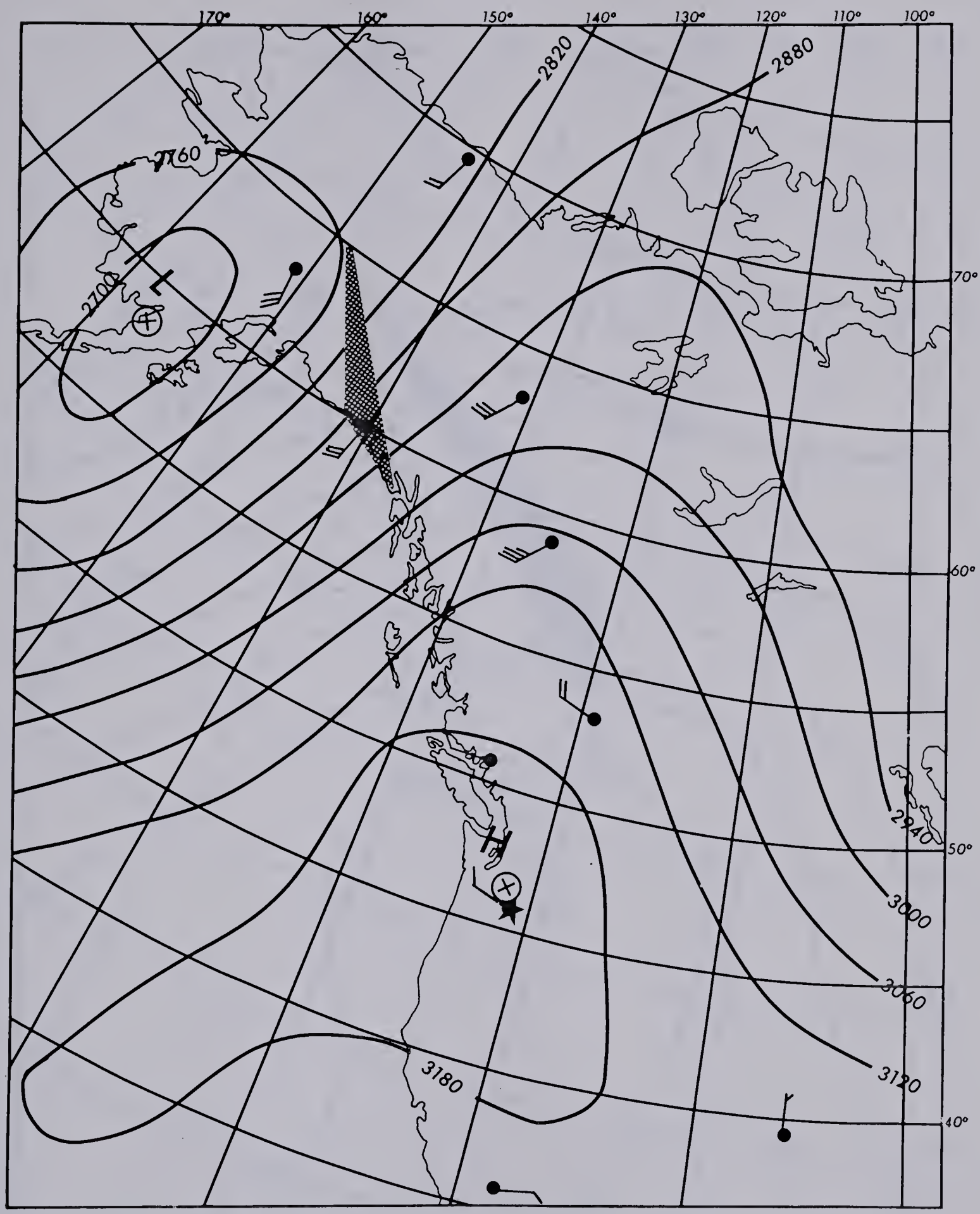

Case 3 700 mb 00Z 08 Oct 71

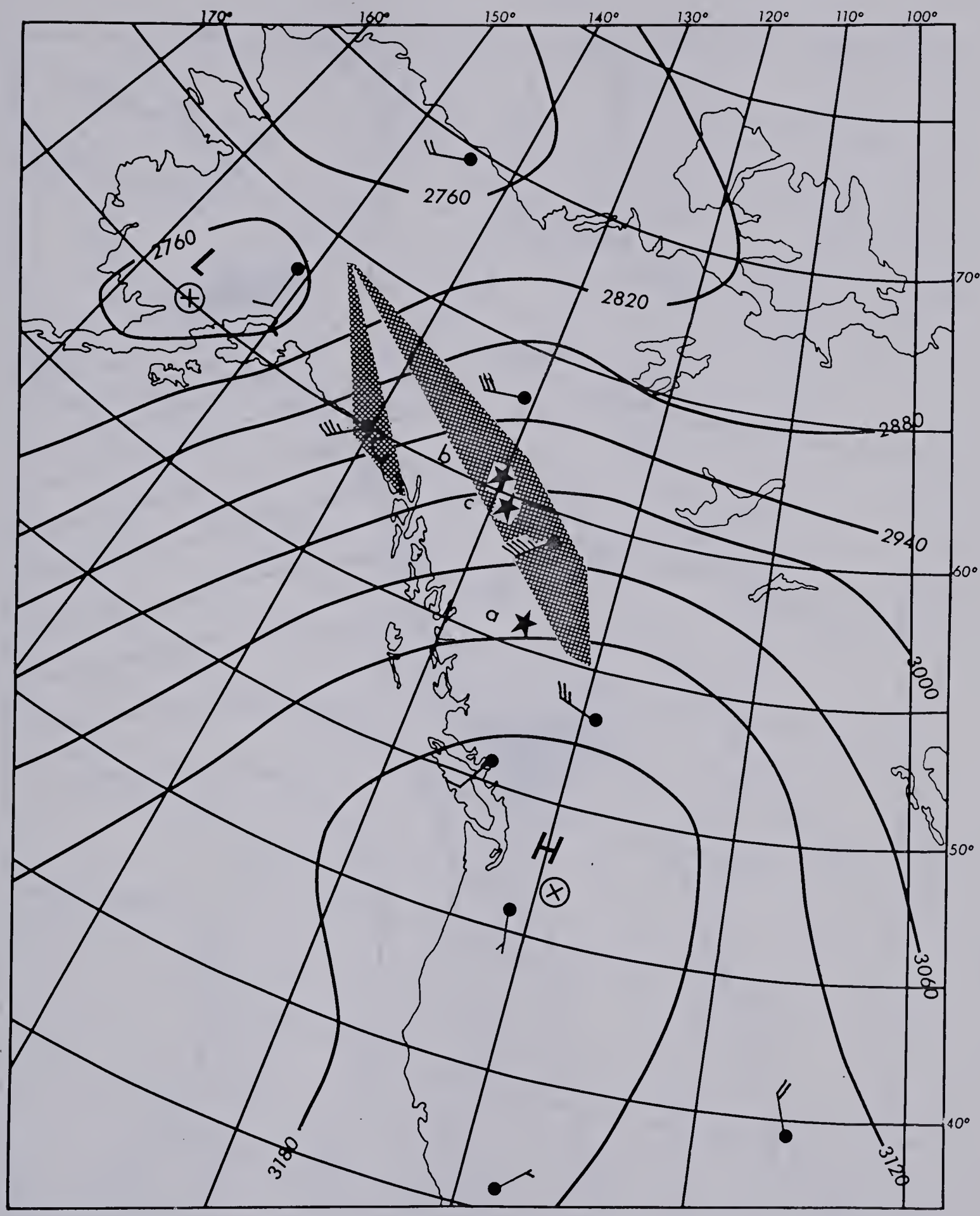

Case 4 700 mb 00Z 09 Oct 71

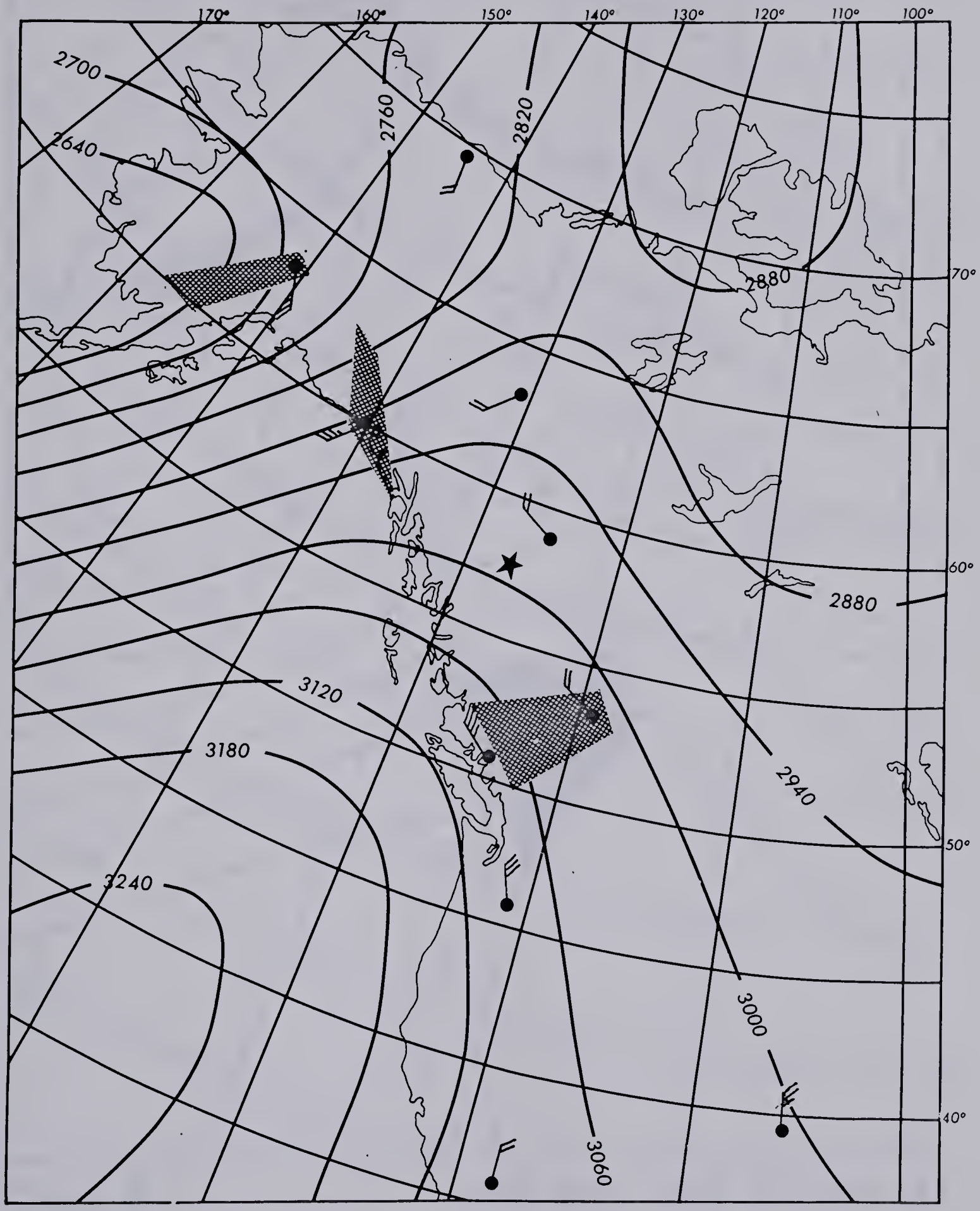

Case 5 700 mb 00Z 18 Nov 71

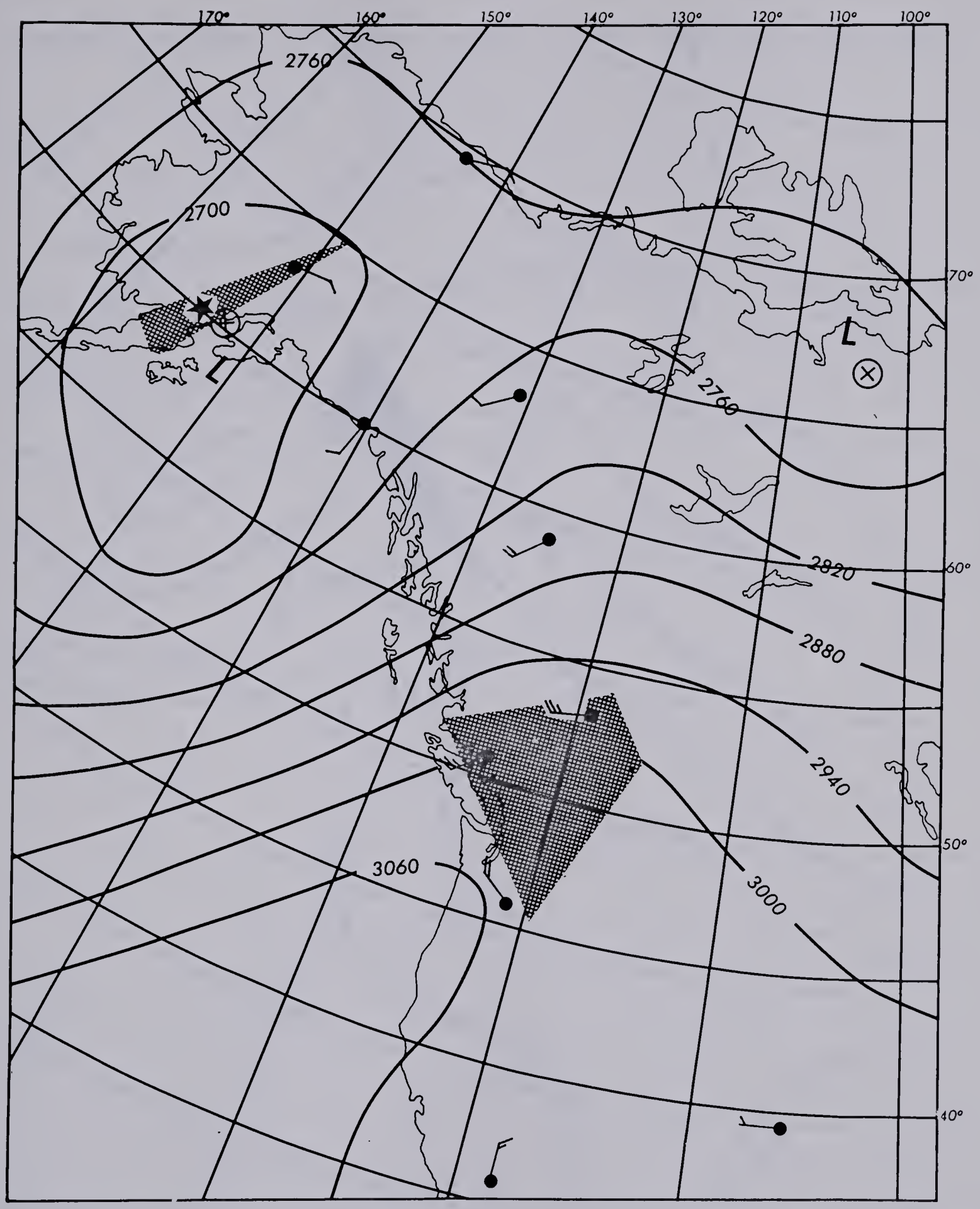

Case 6 700 mb 00Z 01 Dec 71

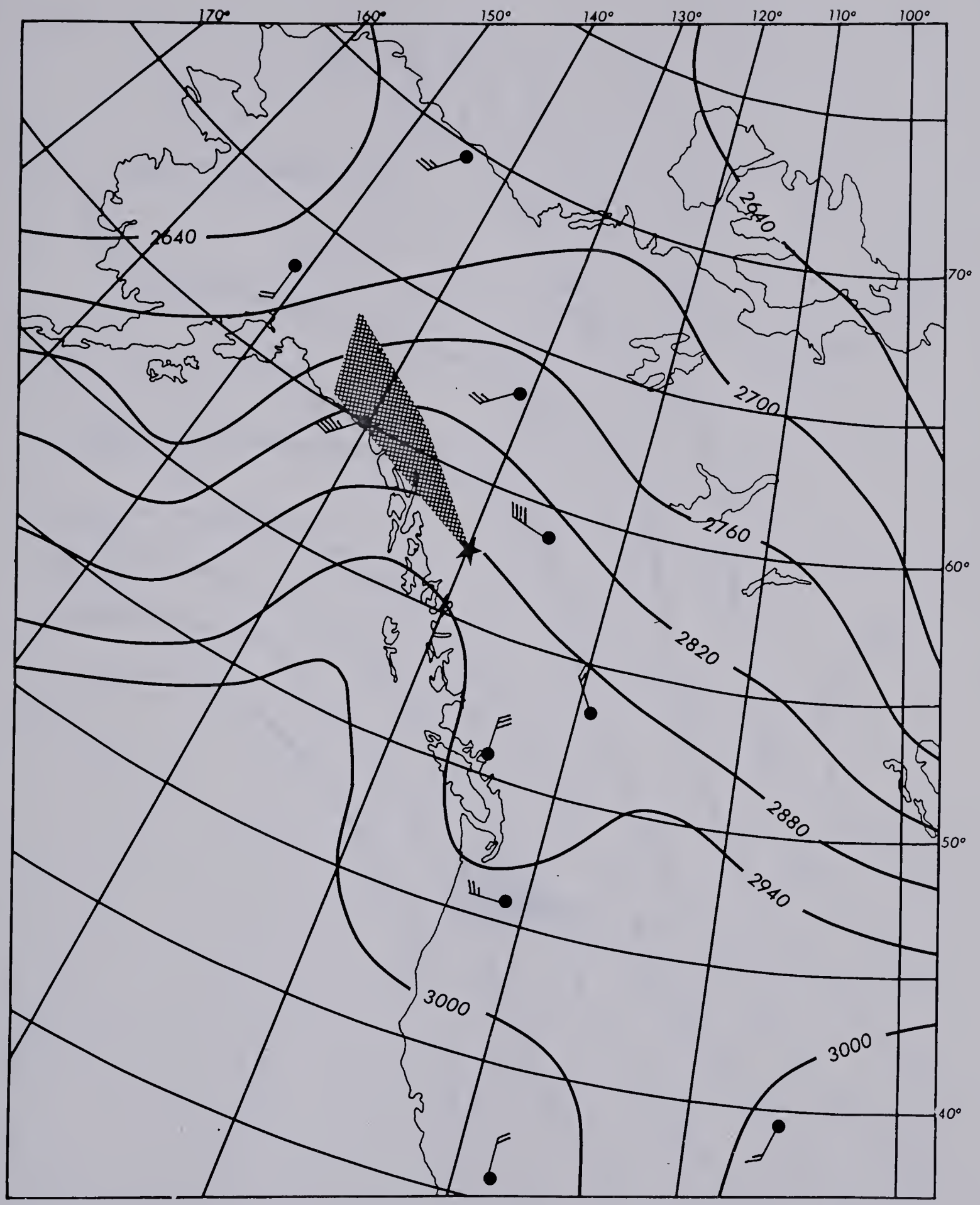

Case 7 700 mb 00Z 29 Dec 71

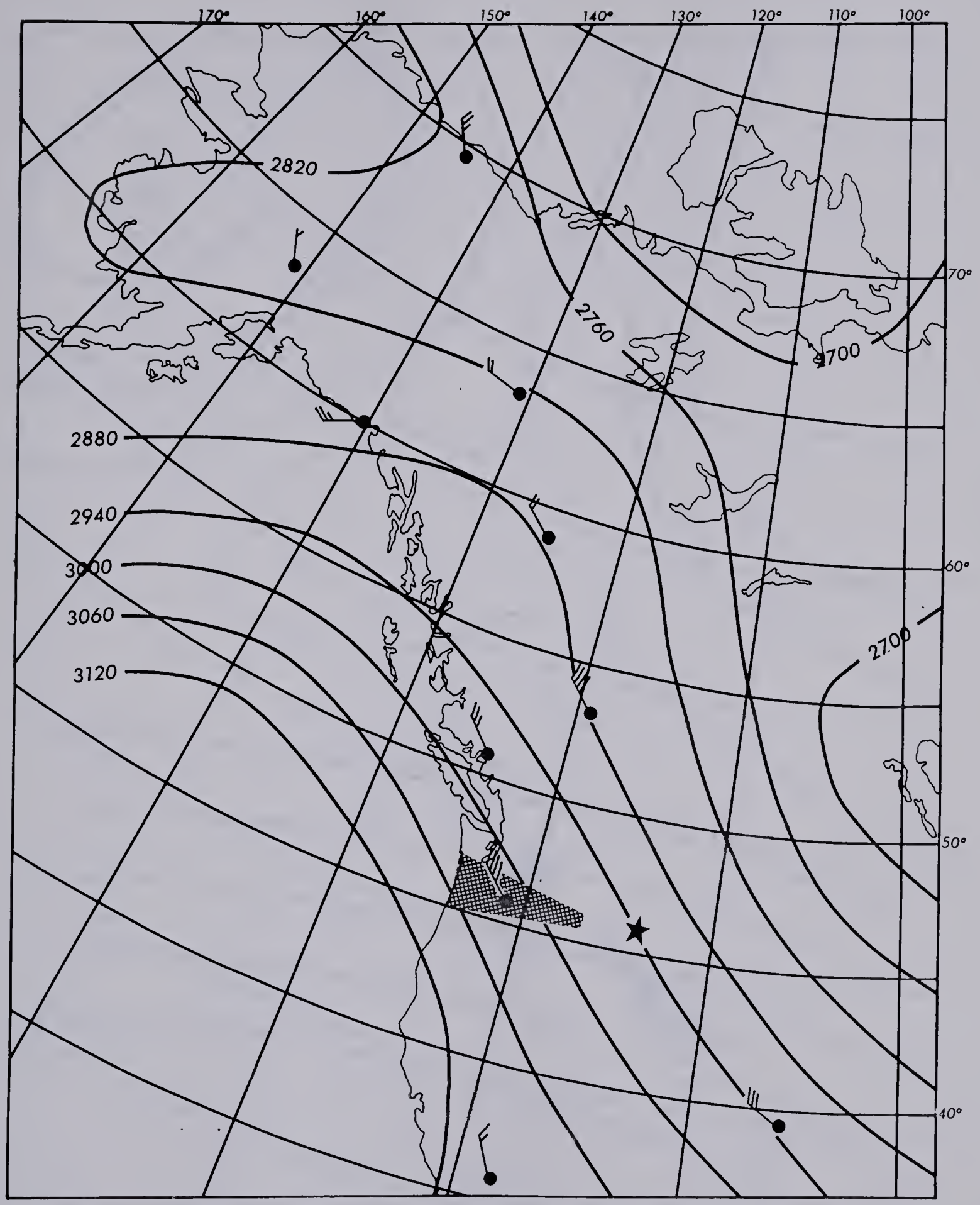

Case 8 700 mb 00Z 14 Jan 72

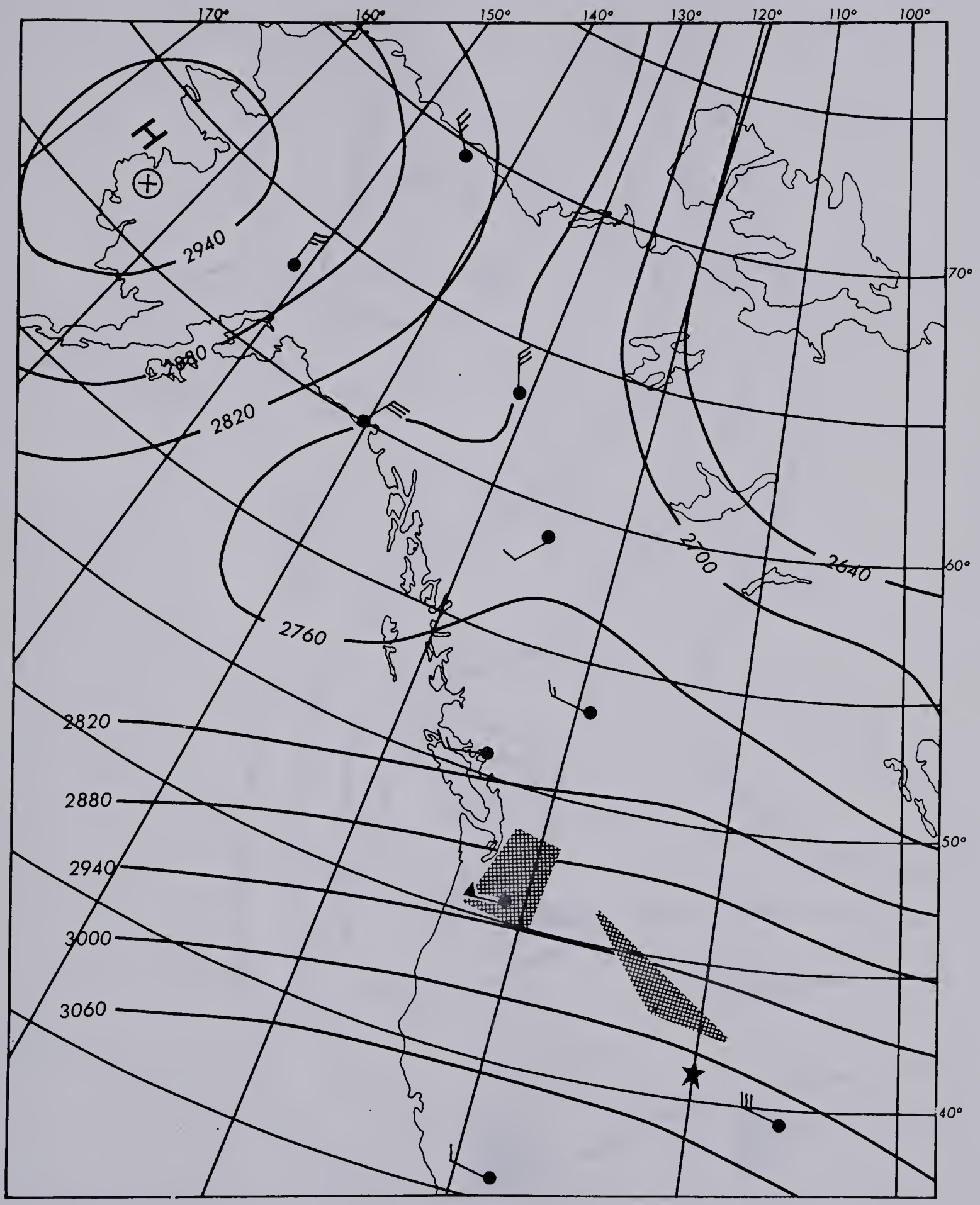

Case 9 700 mb 12Z 18 Jan 72

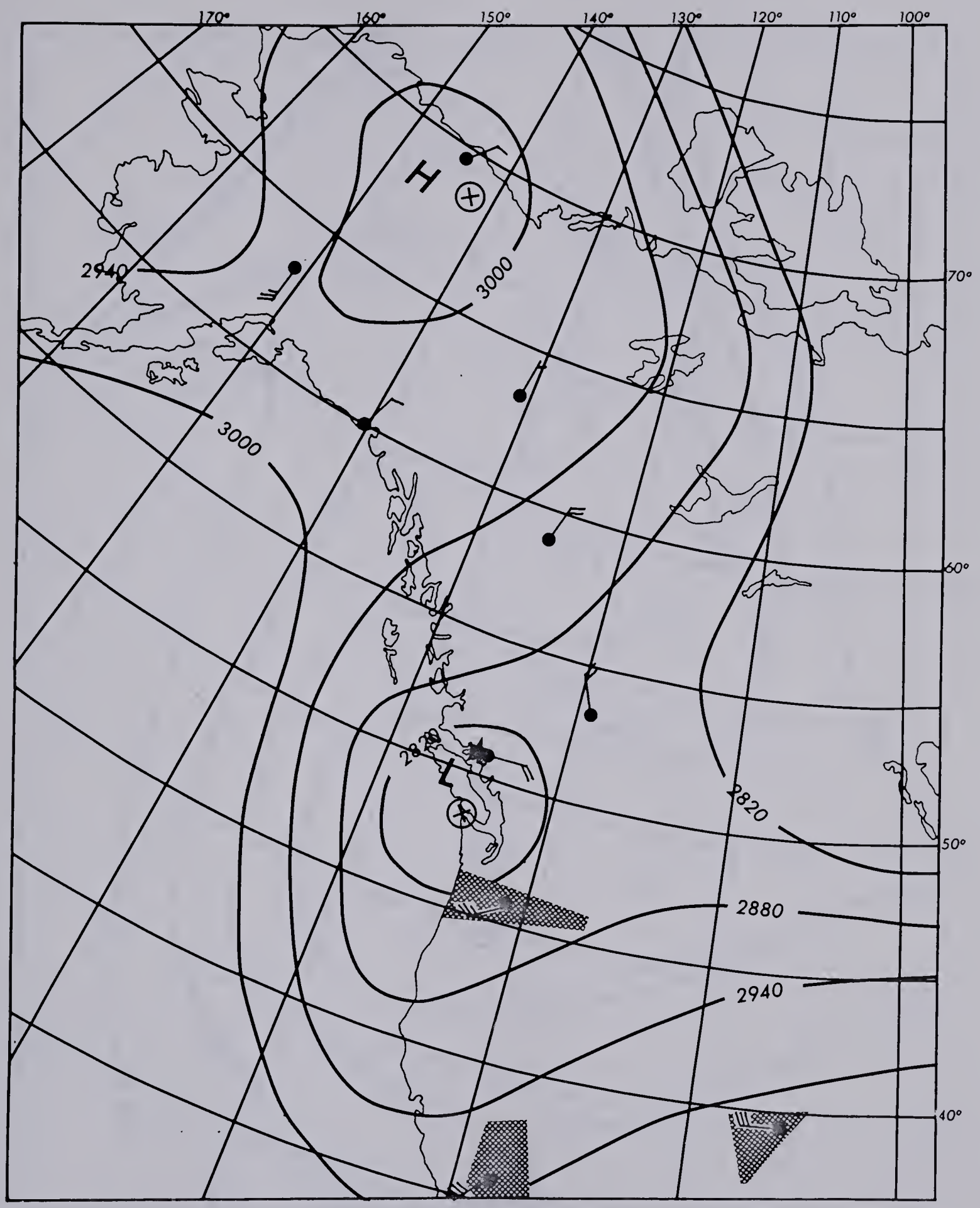

Case 10 700 mb 12Z 25 Jan 72

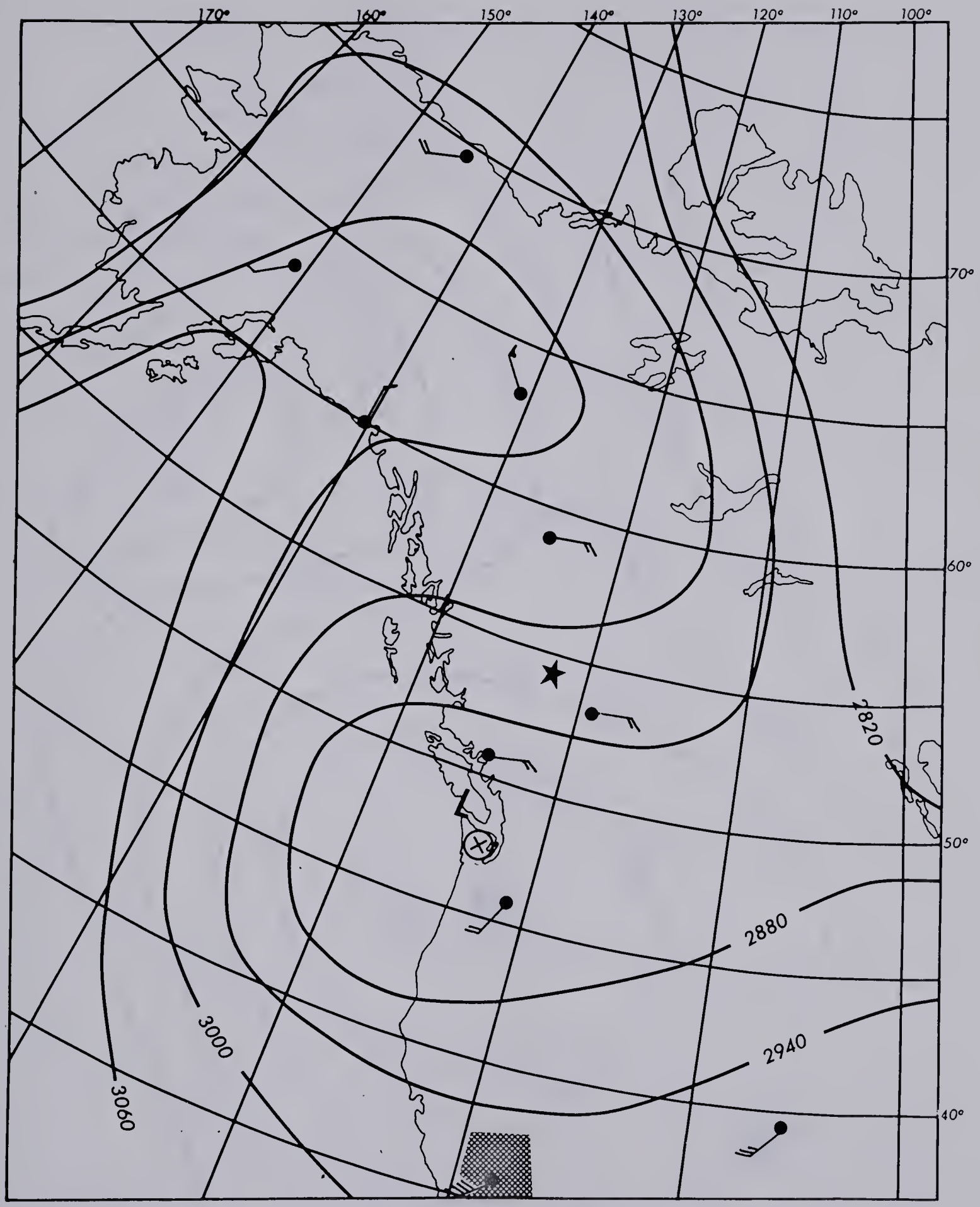

Case 11 700 mb 00Z 26 Jan 72

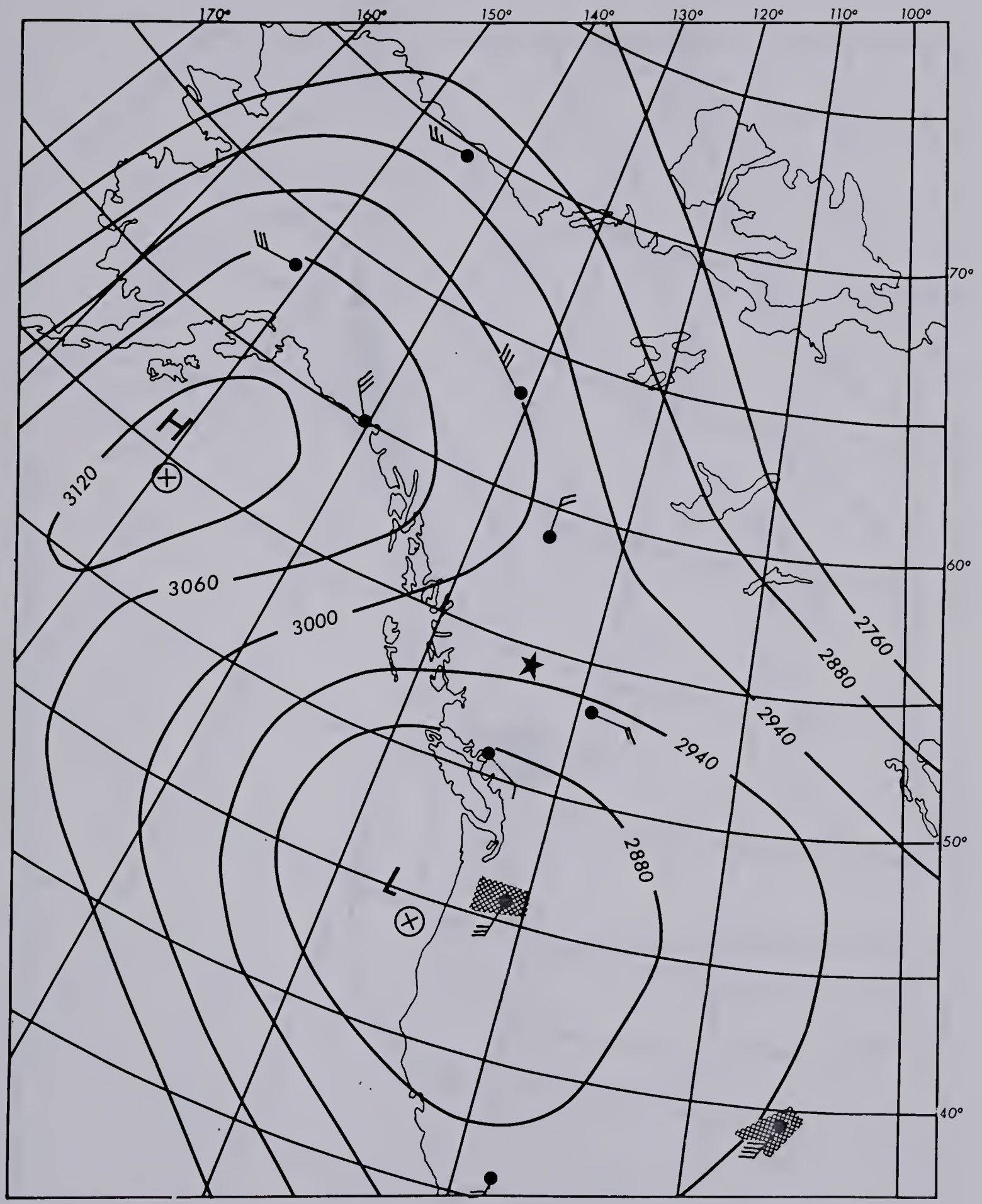

Case 12 700 mb 00Z 27 Jan 72

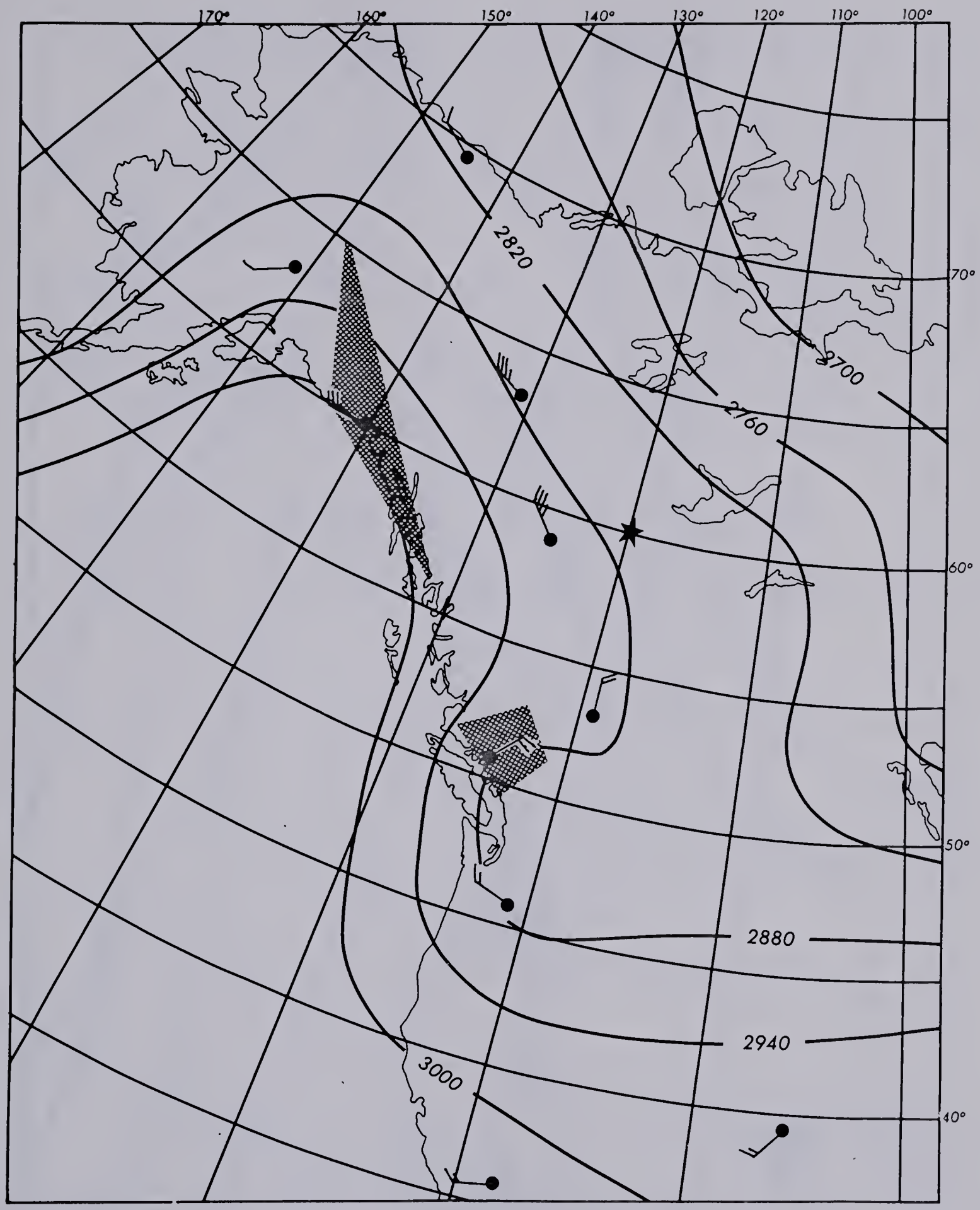

Case 13 700 mb 00Z 01 Feb 72

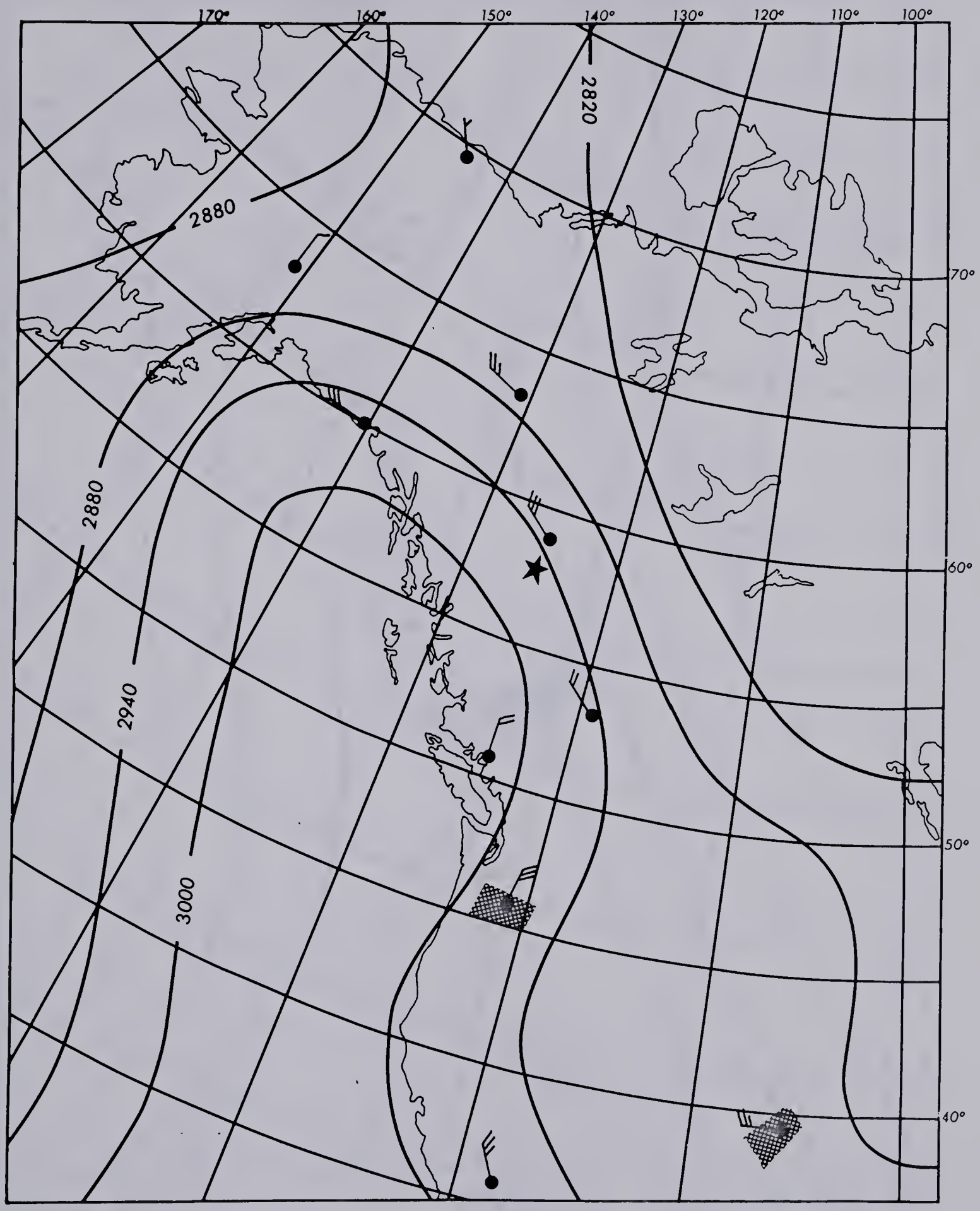

Case 14 700 mb 00Z 02 Feb 72

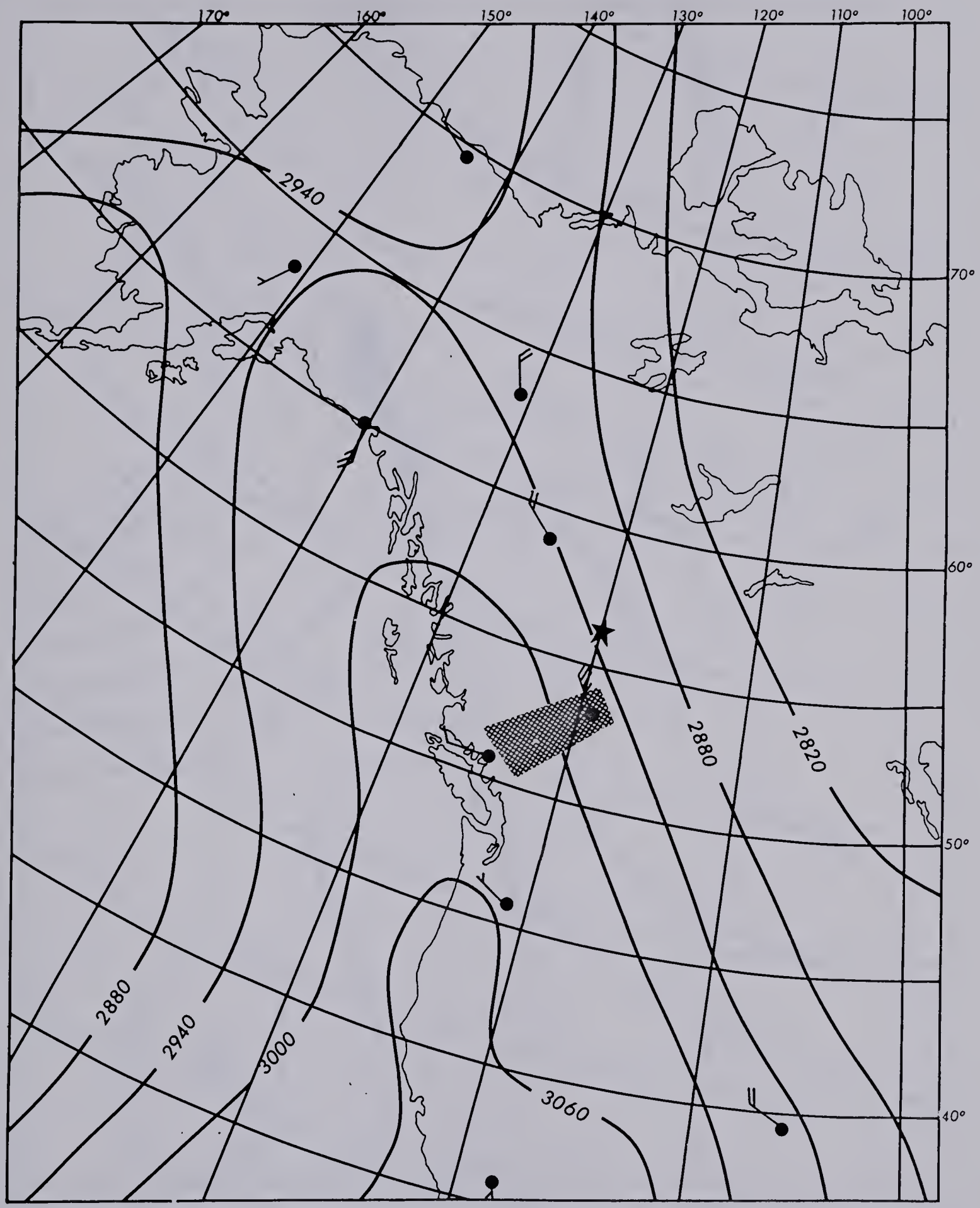

Case 15 700 mb 00Z 03 Feb 72

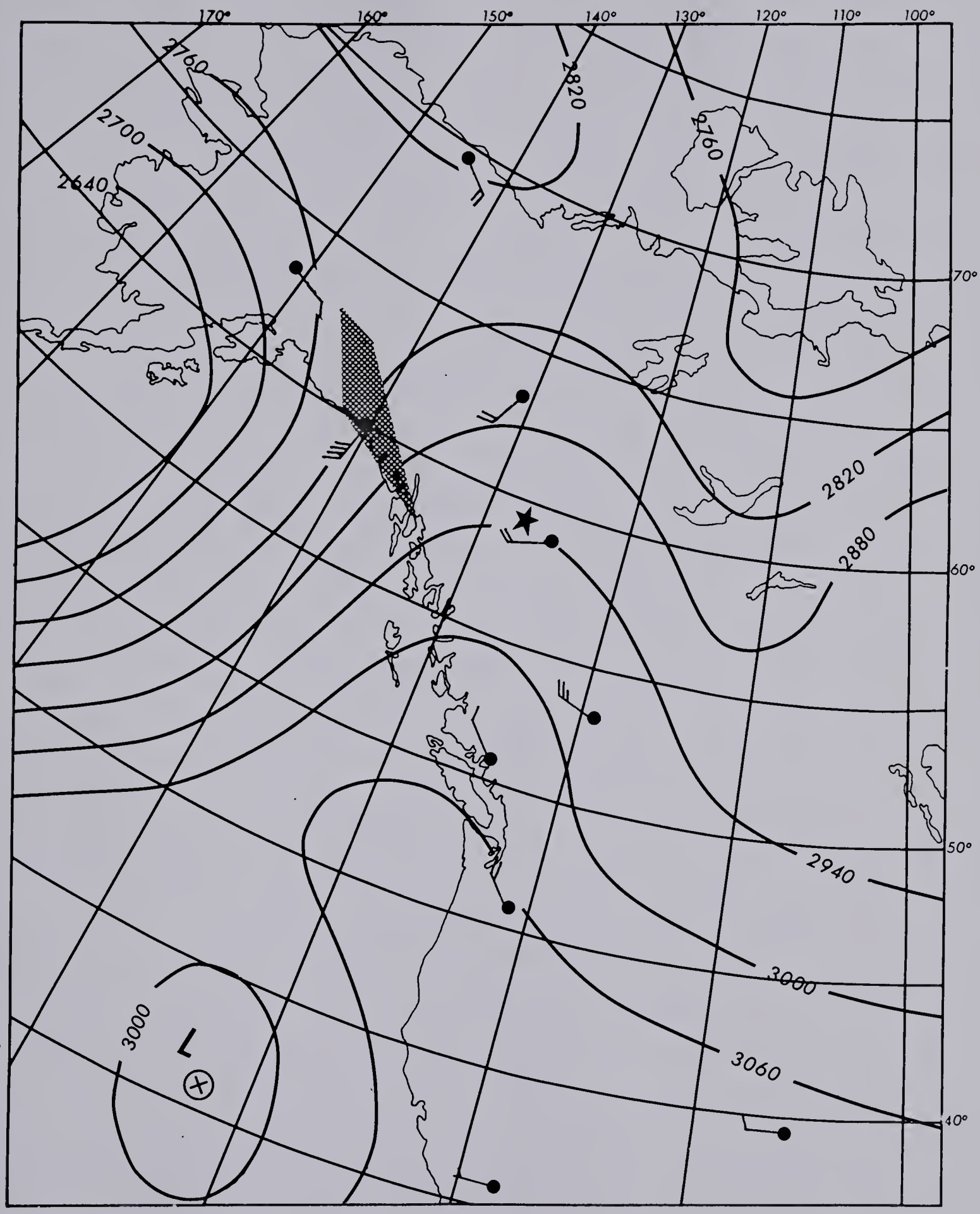

Case 16 700 mb 12Z 09 Feb 72